Zootaxa 5501 (2): 265–290
https://www.mapress.com/zt/

Article

ISSN 1175-5326 (print edition)
ZOOTAXA
ISSN 1175-5334 (online edition)

https://doi.org/10.11646/zootaxa.5501.2.3
http://zoobank.org/urn:lsid:zoobank.org:pub:73F1C13C-D43B-4DCC-9E05-EB9A5B59A776

Akarotaxis gouldae, a new species of Antarctic dragonfish (Notothenioidei: Bathydraconidae) from the western Antarctic Peninsula

ANDREW D. CORSO[1,2*], THOMAS DESVIGNES[3,5], JAN R. MCDOWELL[1,6], CHI-HING CHRISTINA CHENG[4,7], ELLEN E. BIESACK[1,8], DEBORAH K. STEINBERG[1,9] & ERIC J. HILTON[1,10]

[1]*Virginia Institute of Marine Science, William & Mary, Gloucester Point, VA 23062, U.S.A.*
[2]*Present address: Coonamessett Farm Foundation, 277 Hatchville Road, East Falmouth, MA 02536, U.S.A.*
[3]*Institute of Neuroscience, University of Oregon, Eugene, OR 97403, U.S.A.*
[4]*Department of Evolution, Ecology, & Behavior, University of Illinois, Urbana-Champaign, IL 61801.*
[5] *tdesvign@uoregon.edu; https://orcid.org/0000-0001-5126-8785*
[6] *mcdowell@vims.edu; https://orcid.org/0000-0002-4849-0649*
[7] *c-cheng@illinois.edu; https://orcid.org/0000-0001-6308-8685*
[8] *eebiesack@vims.edu; https://orcid.org/0000-0001-7932-9471*
[9] *debbies@vims.edu; https://orcid.org/0000-0001-9884-4655*
[10] *ehilton@vims.edu; https://orcid.org/0000-0003-1742-3467*
**Corresponding author: acorso@cfarm.org; https://orcid.org/0000-0002-8180-3360*

Abstract

Bathydraconidae (Notothenioidei) are a group of benthic fishes endemic to the Southern Ocean. Because of their recent evolutionary radiation and limited sampling efforts due to their occurrence in remote regions, their diversity is likely underestimated. *Akarotaxis nudiceps*, currently the only recognized member of its genus, is an especially poorly known bathydraconid. Although *A. nudiceps* has a circumpolar distribution on the Antarctic continental shelf, its deep habitat and rarity limit knowledge of its life history and biology. Using a combination of morphological and genetic analyses, we identified an undescribed species of this genus, herein named *Akarotaxis gouldae* **sp. nov.** (Banded Dragonfish). The separation of this species was initially identified from archived larval specimens, highlighting the importance of early life stage taxonomy and natural history collections. All currently known adult and larval *A. gouldae* **sp. nov.** specimens have been collected from a restricted ~400 km coastal section of the western Antarctic Peninsula, although this is possibly due to sampling bias. This region is targeted by the epipelagic Antarctic krill fishery, which could potentially capture larval fishes as bycatch. Due to the extremely low fecundity of *A. gouldae* **sp. nov.** and near-surface occurrence of larvae, we suggest the growing Antarctic krill fishery could negatively impact this speces.

Key words: *Bathydraco*ninae, cryonotothenioid, Notothenioid, Bellingshausen Sea, Southern Ocean, krill fishing, Antarctica

Introduction

Notothenioidei are a suborder of Perciformes comprising eight families and about 140 species found throughout the Southern Ocean and nearby waters (Eastman & Eakin 2021). They form a unique radiation of fishes, representing one of the few recognized examples of a marine species flock (Lecointre *et al.* 2013), resulting from their recent endemic speciation and the oceanographic barriers of the Southern Ocean (Eastman & McCune 2000). Some notothenioid species, such as *Notothenia coriiceps* Richardson 1844, *Harpagifer antarcticus* Nybelin 1947, and *Chaenocephalus aceratus* (Lönnberg 1906), have been relatively well documented for their life history (Novillo *et al.* 2019; Postlethwait *et al.* 2016), sensitivity to stressors (O'Brien *et al.* 2018; Saravia *et al.* 2021), and genetics (Beck *et al.* 2022; Bilyk *et al.* 2019), in part because of their abundance and past exploitation, their occupation of relatively shallow coastal habitats, and research interest in their unique physiological adaptations. However, the diversity and biology of rare and deep-dwelling notothenioid taxa remain poorly understood. The presence of cryptic diversity among notothenioids has recently been reported (Ceballos *et al.* 2019; Dornburg *et al.* 2016). Sub-

Accepted by G. Short: 12 Jun. 2024; published: 30 Aug. 2024

Antarctic islands, such as South Georgia, likely contain higher proportions of cryptic species compared to Antarctica because they may have served as habitat refugia during glacial maxima and subsequently as source populations during periods of glacial retreat (Dornburg *et al.* 2016, 2017). However, it is also possible that the deepest regions of the continental shelf functioned as refugia, which could harbor unknown diversity in these hard-to-sample areas (Dornburg *et al.* 2016; Riddle *et al.* 2007).

Bathydraconidae, or Antarctic dragonfishes, are a notothenioid family first defined by Regan (1913) and now comprising 16 valid species (Eastman & Eakin 2021). Many of these species occur at depths greater than 500m, are small, and are rarely collected (Eastman 2017; Gon & Heemstra 1990), thus little is known about their biology, morphology, or population structure. Recent studies have focused on testing the monophyly of Bathydraconidae with respect to the Channichthyidae (Derome *et al.* 2002; Near *et al.* 2018), describing their biology (Barrera-Oro & Lagger 2010; Kuhn *et al.* 2011; La Mesa *et al.* 2018; Novillo *et al.* 2018), and on early life stages and biogeography (La Mesa *et al.* 2017; Desvignes *et al.* 2020; Corso *et al.* 2023).

The bathydraconid genus *Akarotaxis* (DeWitt & Hureau 1980) currently contains a single recognized species, *A. nudiceps* (Waite 1916), which is known from the Bellingshausen, Weddell, Lazarev, Cooperation, Davis, D'Urville, Ross, and Amundsen seas (Cao *et al.* 2022; Duhamel *et al.* 2014; Ekau 1990; Gon & Heemstra 1990; La Mesa *et al.* 2019), suggesting a circumpolar distribution on the Antarctic continental shelf (Fig. 1). Although most adult specimens of this species are from collections made over bottom depths ranging from 370 to 600 m, specimens of *A. nudiceps* have been collected as deep as 1191 m (Eastman 2017). Due to the extremely low absolute fecundity of *A. nudiceps* (<300 oocytes), La Mesa *et al.* (2007a) suggested that nest guarding is likely. The early life history stages of *A. nudiceps* are also poorly known, likely due in part to their low fecundity, although Corso *et al.* (2023) recently described the pelagic larval stages of *A. nudiceps* based on specimens derived from a long-term monitoring program along the western Antarctic Peninsula (WAP) coast (Fig. 1).

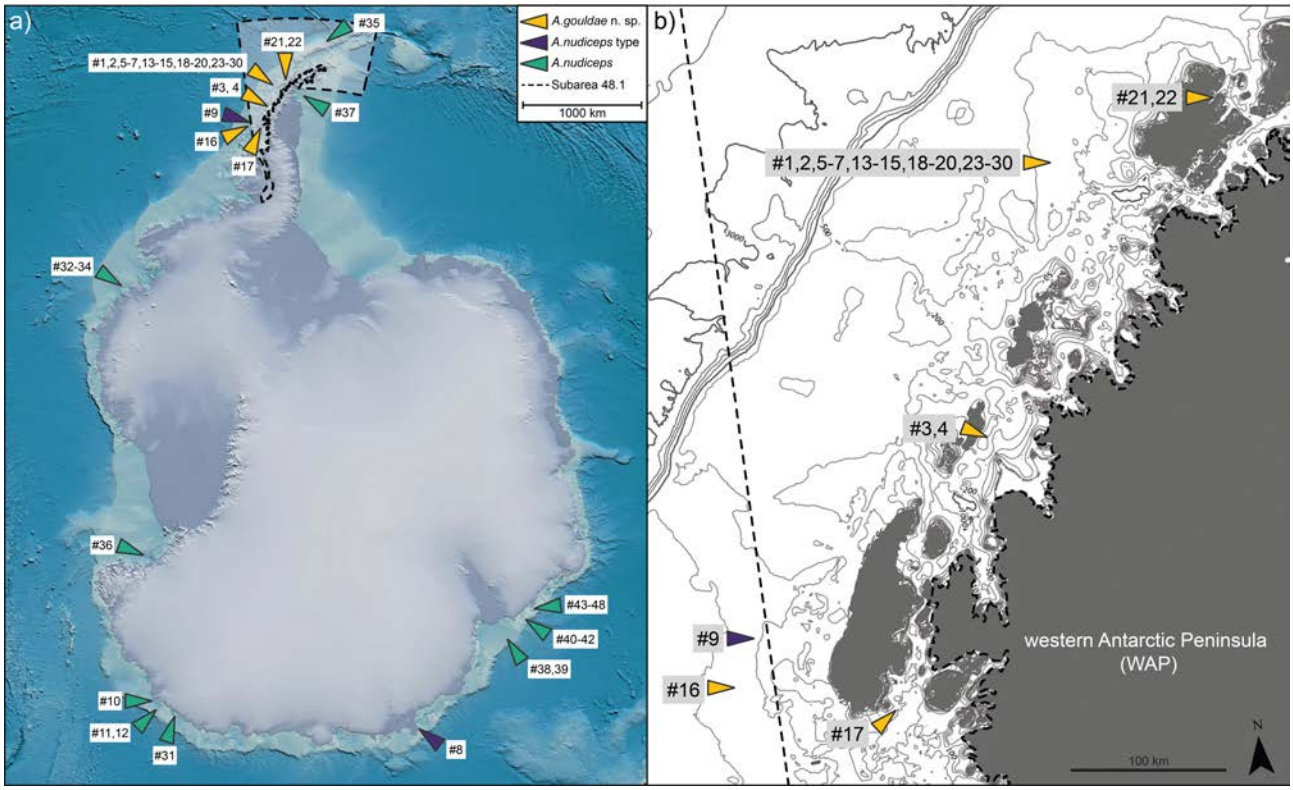

FIGURE 1. Maps of a) all collection sites of specimens of *Akarotaxis* spp. referred to in this study, with *A. gouldae* **sp. nov.** marked by yellow arrows, the type specimens of A. *nudiceps* (#8, #9) by purple arrows, and all other A. *nudiceps* marked by green arrows. b) a magnified visualization of all known *Akarotaxis gouldae* **sp. nov.** collection sites near the western Antarctic Peninsula (WAP), with bathymetric information in meters. In both maps, numbers associated with each location correspond to the Label # in Tables 1 and 3. The CCAMLR subarea 48.1 is shown by a dashed line.

As part of the larval description of *Akarotaxis nudiceps*, Corso *et al.* (2023) sequenced two mitochondrial markers (*mt-nd2* and *mt-co1*) from two larval specimens identified as *A. nudiceps* collected in the Bellingshausen Sea (Fig. 1). Several nucleotide differences were noted between sequences from these specimens and sequences from specimens collected in other areas of the Southern Ocean, suggesting that the larvae represented either a distinct population or a separate species. In this study, we further explored these differences by combining morphological and genetic analyses of additional specimens, ultimately demonstrating the presence of a previously undescribed species of dragonfish in the genus *Akarotaxis*.

Materials and Methods

Morphological analysis

Specimens for morphological analysis are from the collections of the Nunnally Ichthyology Collection at the Virginia Institute of Marine Science, William & Mary, Gloucester Point, Virginia, USA (VIMS), the Collection d'Ichthyologie at the Muséum national d'Histoire naturelle, Paris, France (MNHN), Oregon State University Ichthyology Collection, Corvallis, Oregon, USA (OS), and the Peabody Museum of Natural History at Yale University, New Haven, Connecticut, USA (YPM ICH). Digital images and x-rays of two paratype specimens, AMS IA.484 and AMS IA.485, of *A. nudiceps* were obtained from Australian Museum, Sydney, N. S. W., Australia (AMS). Collection abbreviations follow Sabaj (2020). Information about the specimens used in the morphological analyses is provided in Table 1.

TABLE 1. Collection information of *Akarotaxis* spp. specimens examined morphologically in this study (*A. gouldae* **sp. nov.** and *A. nudiceps*). We were unable to measure the holotype for A. nudiceps (#8) and the genus *Akarotaxis* (#9) directly, but used measurements published in Dewitt & Hureau (1980).

Label #	Species	Voucher ID	SL (mm)	Collection date	Capture Location	Depth (m)	Latitude	Longitude
1	*A. gouldae* **sp. nov.** (holotype)	YPM ICH 24241	140.8	22-Apr-2010	Hugo-Anvers Trough, WAP	675	-64.739	-65.433
2	*A. gouldae* **sp. nov.**	YPM ICH 36536	135.8	22-Apr-2010	Hugo-Anvers Trough, WAP	675	-64.739	-65.433
3	*A. gouldae* **sp. nov.**	YPM ICH 20043	129.3	15-May-2008	Banana Trench, WAP	692	-66.266	-66.546
4	*A. gouldae* **sp. nov.**	YPM ICH 20045	127.3	15-May-2008	Banana Trench, WAP	692	-66.266	-66.546
5	*A. gouldae* **sp. nov.**	VIMS 45856	136	9-May-2018	Hugo-Anvers Trough, WAP	698-700	-64.753	-65.505
6	*A. gouldae* **sp. nov.**	OS 26108	133	20-Aug-2017	Hugo-Anvers Trough, WAP	690-705	-64.746	-65.481
7	*A. gouldae* **sp. nov.**	OS 26109	133	20-Aug-2017	Hugo-Anvers Trough, WAP	690-705	-64.746	-65.481
8	*A. nudiceps* (holotype)	SAM F-369	119	28-Jan-1914	Shackleton Ice Shelf	439	-65.330	95.450
9	*A. nudiceps* (paratype)	UMOD 148-1	129	26-Feb-1972	Adelaide Island, WAP	630-650	-67.260	-70.200
10	*A. nudiceps*	MNHN-2009-1057	105.2	31-Dec-2007	D'Urville Sea	839-860	-66.737	144.640
11	*A. nudiceps*	MNHN-2009-1074	117.3	4-Jan-2008	D'Urville Sea	689-710	-66.316	143.301
12	*A. nudiceps*	MNHN-2009-1075	97.2	4-Jan-2008	D'Urville Sea	689-710	-66.316	143.301

We used Mitutoyo 500-752-20 digital calipers for all measurements, which were recorded to the nearest 0.01 mm. We followed the methods of DeWitt & Hureau (1980), in which measurements are defined as follows and illustrated in Figure 2: standard length (SL; from the tip of the upper jaw to the posterior end of the hypural bone), head length (HL; from the tip of the upper jaw to the posterior tip of the operculum), head width (HW; widest point of the head), head depth (HD; distance from dorsal to ventral sides of head at mid-orbit), orbital diameter (O; greatest horizontal distance between the eye socket rims), snout length (SnL; from the tip of the upper jaw to the most anterior margin of the orbit), interorbital width (IO; the shortest distance between the dorsal margins of the orbital rim at mid-orbit), upper jaw length (UJL; from tip of upper jaw to posterior end of maxilla), caudal peduncle length (CPL; posterior insertion of dorsal fin to the posterior end of the hypural bones), caudal peduncle depth (CPD; from the dorsal to ventral sides of caudal peduncle at the widest point), body depth [BD(AO); from the dorsal to ventral sides of the body at the anterior origin of the anal fin], predorsal-fin distance (Sn-D; from the tip of the upper jaw to the anterior origin of the dorsal fin), preanal-fin distance (Sn-AO; from the tip of the upper jaw to the anterior origin of the anal fin), distance between anal-fin origin and caudal-fin base (AO-C; anterior origin of anal fin to the posterior end of the hypural bones), distance between pelvic-fin base and anal-fin origin (AO-V; anterior origin of anal fin to the anterior base of the pelvic fin), pectoral-fin length (PL; base to tip of fin rays with preference for the left side if available), pelvic-fin length (VL; base to tip of fin rays; on the left side if available), caudal-fin length (CL; distance from posterior end of the hypural bones to the tip of the fin rays). Mean (± standard deviation) for each measurement are reported in Table 2.

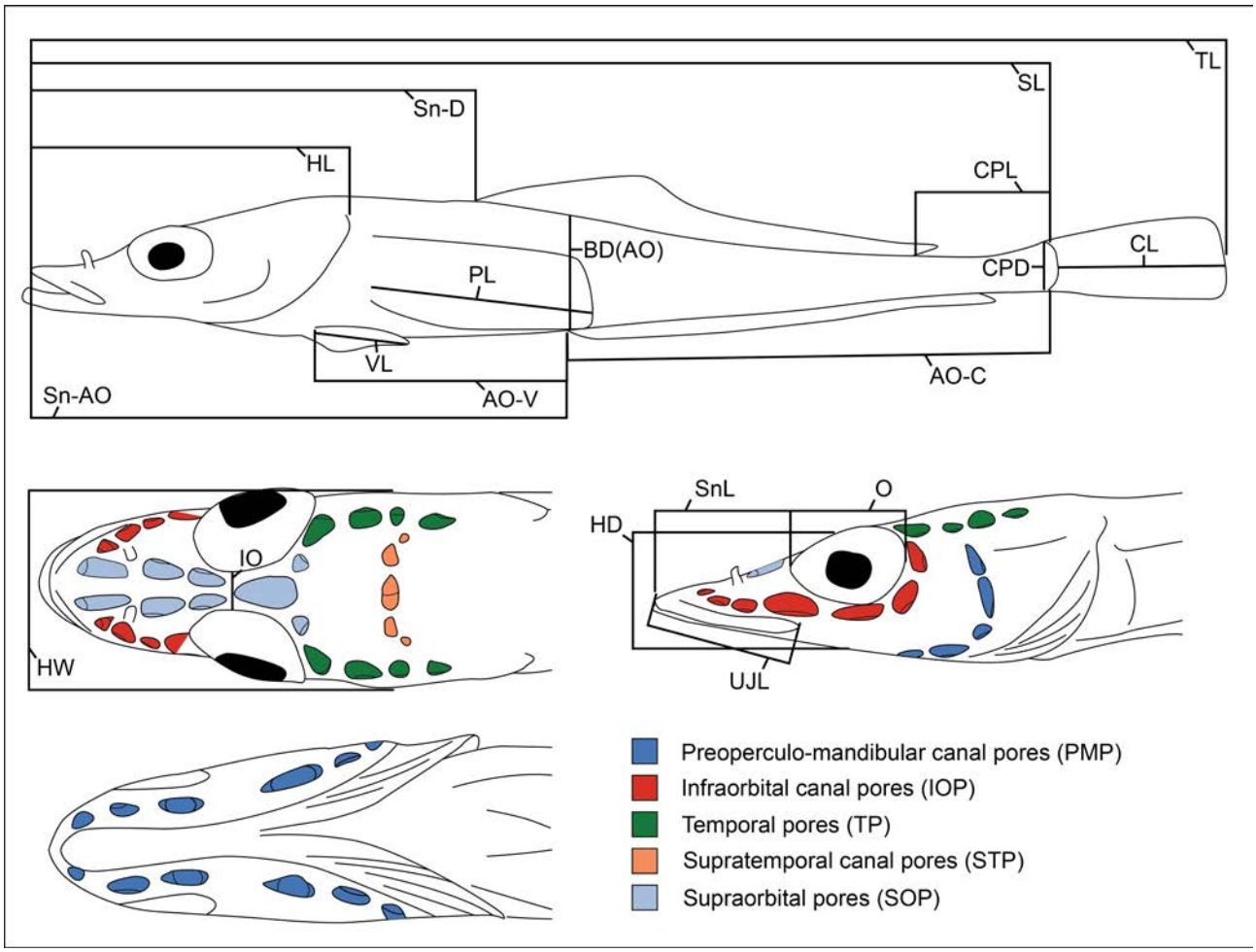

FIGURE 2. Measurements used in this study depicted on an illustration of *A. gouldae* **sp. nov.**, including standard length (SL), head length (HL), head width (HW), head depth (HD), orbital diameter (O), snout length (SnL), interorbital space (IO), jaw length (UJL), caudal-peduncle length (CPL), caudal peduncle depth (CPD), body depth [BD(AO)], predorsal-fin distance (Sn-D), preanal-fin distance (Sn-AO), distance between anal-fin origin and caudal-fin base (AO-C), distance between pelvic-fin base and anal-fin origin (AO-V), pectoral-fin length (PL), pelvic-fin length (VL), caudal-fin length (CL). Large bony vacuities enclosed by a thin membrane (i.e., pores) found on the heads of *Akarotaxis* spp. are colored according to their names

TABLE 2. Mean (± Standard Deviation) and ranges of meristic information of all *Akarotaxis* spp. specimens listed in Table 1. Means are reported as a percentage of standard length (SL). Meristic data highlighted in the manuscript are italicized. Meristics for *A. nudiceps* type specimens are from Dewitt & Hureau (1980). Vertebral counts (abdominal and caudal) for type specimens of *A. nudiceps* were not available and are based on the paratypes AMS IA.484 and AMS IA.485 (see Remarks).

Specimen Group	***A. gouldae* sp. nov. (n=7)**	***A. nudiceps* type specimens (n=2)**	***A. nudiceps* (n=3)**
	Mean (+/- SD)	Mean (+/- SD)	Mean (+/- SD)
Standard length (SL)	131.7 ± 5.4	124 ± 7.1	106.6 ± 10.1
Head length (HL)	33.3 ± 1.0	33.9 ± 2.7	33.8 ± 0.9
Head width (HW)	14.2 ± 0.4	15.9 ± 3.2	14.3 ± 0.6
Head depth (HD)	10.5 ± 1.4	12.5 ± 2.1	9.5 ± 0.8
Orbital diameter (O)	9.0 ± 0.4	9.4 ± 1.3	8.4 ± 0.5
Snout length (SnL)	10.3 ± 0.4	10.6 ± 0.9	11.0 ± 0.1
Interorbital space (IO)	2.7 ± 0.3	2.6 ± 0.4	3.1 ± <0.0
Jaw length (UJL)	10.7 ± 0.5	11.8 ± 1.8	11.3 ± 0.2
Caudal-peduncle length (CPL)	7.7 ± 0.3	7.0 ± 0.8	6.7 ± 1.0
Caudal peduncle depth (CPD) max	4.1 ± 0.8	3.4 ± 0.1	5.0 ±0.7
Body depth [BD(AO)]	12.7 ± 2.7	10.5 ± 0.4	8.8 ± 0.3
Predorsal-fin distance (Sn-D)	42.1 ± 1.3	44.2 ± 3.1	44.9 ± 0.3
Preanal-fin distance (Sn-AO)	53.2 ± 2.3	53.4 ±3.4	53.3 ± 0.4
Dist. between A origin and C base (AO-C)	47.2 ± 1.2	43.9 ± 1.6	46.7 ± 0.8
Dist. between V base and A origin (AO-V)	25.0 ± 1.4	24.7 ± 0.3	23.1 ± 1.1
Pectoral length (PL)	21.7 ± 1.6	23.8 ±1.6	22.8 ± 1.0
Pelvic length (VL)	19.1 ± 0.8	21.0 ± 0.5	19.9 ± 2.0
Caudal length (CL)	15.0 ± 0.6	17.9 ± 0.4	15.3 ± 1.2
Orbital diameter / snout length (O/SnL)	87.7 ± 4.4	88.9 ± 4.3	76.5 ± 5.2
Snout length / head length (SnL/HL)	30.9 ± 1.2	31.1 ± 0.2	32.6 ± 1.2
Jaw length / head length (UJL/HL)	32.0 ± 1.5	34.7 ± 2.7	33.5 ± 0.5
	Range	**Range**	**Range**
Anterior gill rakers (Ant GR)	(7-9) + 0 + (18-20)	9 + 0 + (19-20)	(7-8) + 0 + (17-21)
Posterior gill rakers (Post GR)	(3-4) + 0 + (14-18)	4 + (0-1) + (17-18)	(3-4) + 0 + (14-15)
Dorsal fin rays (D)	28–31	33–31	27–28
Anal fin rays (A)	25–28	27–28	24–25
Caudal fin rays (C)	12–13	12–13	12
Pectoral fin rays (P)	20–22	22–23	21
Middle lateral line scales (MLL)	84–91	86–88	71–74
Upper lateral line scales (ULLt)	3–5t	4–5t	4–6t
Branchiostegal rays (Br)	6	6	6
Preoperculo-mandibular canal pores (PMP)	(8-9) / (7-9)	8 / 8	(7-9) / (7-8)
Infraorbital canal pores (IOP)	7 / 7	7 / 7	7 / 7
Supraorbital pores (SOP)	4 + 1 + 4	(3-4) + 0 + (3-4)	4 + 1 + 4
Temproal pores (TP)	4 / 4	(3-5) / (3-4)	4 / 4
Supratemporal canal pores (STP)	5–6	3	5–6
Abdominal vertebral	16–17	16–17*	16–17
Caudal vertebral	31–33	31–32*	31

In addition to measurements, we also collected meristic data following DeWitt & Hureau (1980), including: anterior gill rakers (Ant GR; leading edge of first arch), posterior gill rakers (Post GR; trailing edge of first arch), dorsal-fin rays (D), anal-fin rays (A), caudal-fin rays (C), pectoral-fin rays (P), tubular scales along the upper lateral line (ULLt), scales along the middle lateral line (MLL), branchiostegal rays (Br). We also counted preoperculomandibular canal pores (PMP), infraorbital canal pores (IOP), supraorbital pores (SOP), temporal pores (TP), and supratemporal canal pores (STP) which are illustrated in Figure 2. Pores are reported as bilateral counts, except for STP, which are reported as total counts. Ranges for counts are reported in Table 2.

Mapping of catch sites

Maps were created in ArcGIS Pro (Version 3.1.1, Environmental Systems Research Institute) with bathymetry data from the International Bathymetric Chart of the Southern Ocean Version 2 (Dorschel *et al.* 2022). The Commission for the Conservation of Antarctic Marine Living Resources (CCAMLR) provided data to map Subarea 48.1 (Fig. 1).

Fecundity data

One gravid female (Label #14, SL = 153 mm, Total weight = 29.93 g) was dissected to estimate fecundity and reproductive investment. This specimen was captured on 08-20-2017 in Hugo-Anvers Trough and was originally identified as *A. nudiceps*. Fresh ovaries weighing 5.1 g were fixed intact in Bouin's fixative. After fixation, the ovaries weighed 3.536 g. A portion of one ovary (0.384 g) was separated, rinsed in 70% ethanol, and oocytes of all stages were dissociated and imaged on a Leica M165 FC stereomicroscope equipped with a Leica DFC425 C digital camera. Absolute fecundity was estimated by scaling the number of developing (i.e., late vitellogenic) oocytes counted in the studied fragment to the entire gonad weight. Egg diameter was measured using ImageJ and egg size distribution was studied using R.

Mitochondrial DNA amplification and sequencing

We sequenced three mitochondrial gene regions—the full length of NADH dehydrogenase 2 (*mt-nd2*), and a portion of each cytochrome c oxidase I (*mt-co1*) and cytochrome b (*mt-cyb*) from a total of 23 specimens of *Akarotaxis* captured from WAP coastal sites. Specimen and catch locations are detailed in Table 3. DNA from six specimens from the YPM and VIMS collections were isolated and purified with magnetic beads following Corso *et al.* (2023). DNA from 17 individuals from the University of Illinois and University of Oregon (vouchers not retained for the majority of them, see Table 3) captured from Lapeyrere Bay and Anvers-Hugo Trough were isolated using Qiagen DNeasy Blood and Tissue Kit (Hilden, Germany). PCR amplification of the three mitochondrial gene sequences utilized published primer sets (primer sequences and references in Appendix 1; Desvignes *et al.* 2019; Ivanova *et al.* 2007; Kocher *et al.* 1995; Matschiner *et al.* 2011) and Qiagen's Taq Core PCR kit. PCR amplicons were purified, Sanger sequenced using BigDye Terminator v.3.1 Cycle Sequencing chemistry (Applied Biosciences, USA), and electrophoresed on an ABI 3500 or 3730xl capillary sequencer. The sequence reads were edited and assembled using Sequencher 5.3.6 (Gene Codes Corp., USA) or ChromasPro (Technelysium, Australia).

Phylogenetic analysis

In addition to the newly generated sequences from the WAP, additional *Akarotaxis* mitochondrial sequences were sourced from GenBank (Table 3). To place the *Akarotaxis* specimens in a phylogenetic context spanning all Antarctic dragonfish species, a sequence of each species was also included when available (Appendix 2). A sequence from *N. coriiceps* served as an outgroup to root the trees. Combined sequences were aligned using MAFFT version 7 webserver (Katoh *et al.* 2019) and trimmed. Sequence alignments were analyzed in a Maximum-Likelihood (ML) framework using ModelTest-NG (Darriba *et al.* 2020) implemented in raxmlGUI 2.0 (Edler *et al.* 2021) to determine

TABLE 3. Collection information of Akarotaxis spp. that were examined genetically. *mt-co1 sequences not publicly available but obtained from the authors of Li *et al.* (2022) (https://doi.org/10.1016/j.dsr2.2022.105140). **Specimen for which a reference genome assembly was created for A. nudiceps (GCA_943590845.1), but is now identified as A. gouldae **sp. nov.**

ID	Species	Label #	Voucher ID, if any	Field ID	Collection date	Capture Location	Depth (m)	Latitude	Longitude	*mt-co1*	*mt-nd2*	*mt-cyb*
1	*A. gouldae* **sp. nov.**	1	YPM ICH 24241	Corso_62	22/04/2010	Hugo-Anvers Trough, WAP	675	-64.739	-65.433	PQ048200	PQ043690	PQ049615
	A. gouldae **sp. nov.**	2	YPM ICH 36536	Corso_63	22/04/2010	Hugo-Anvers Trough, WAP	675	-64.739	-65.433	N/A	N/A	PQ049616
3	*A. gouldae* **sp. nov.**	3	YPM ICH 20043	Corso_61	15/05/2008	Banana Trench, WAP	692	-66.266	-66.546	PQ048206	HQ170108	PQ049614
4	*A. gouldae* **sp. nov.**	4	YPM ICH 20045	Corso_60	15/05/2008	Banana Trench, WAP	692	-66.266	-66.546	PQ048191	HQ170109	PQ049613
7	*A. gouldae* **sp. nov.**	5	VIMS 45856	Aka_18_07	7/05/2018	Hugo-Anvers Trough, WAP	698-700	-64.753	-65.505	PQ048199	PQ043693	N/A
	A. gouldae **sp. nov.**	13	N/A	Aka_17_05**	20/08/2017	Hugo-Anvers Trough, WAP	692-704	-64.747	-65.498	PQ048204	PQ043696	N/A
	A. gouldae **sp. nov.**	14	N/A	Aka_17_06	20/08/2017	Hugo-Anvers Trough, WAP	692-704	-64.747	-65.498	PQ048210	PQ043695	N/A
	A. gouldae **sp. nov.**	15	N/A	Aka_18_03	30/04/2018	Hugo-Anvers Trough, WAP	698	-64.750	-65.500	PQ048207	PQ043694	N/A
	A. gouldae **sp. nov.**	16	VIMS 43571a	Corso_18	14/01/2019	Adelaide Island, WAP	773	-67.522	-70.591	PQ048208	PQ043691	N/A
	A. gouldae **sp. nov.**	17	VIMS 43240	Corso_19	18/01/2020	Adelaide Island, WAP	387	-67.766	-68.241	PQ048201	PQ043690	N/A
	A. gouldae **sp. nov.**	18	N/A	2008_Aka_1_Hugo	23/07/2008	Hugo-Anvers Trough, WAP	600	-64.807	-65.387	PQ048190	PQ043697	N/A
	A. gouldae **sp. nov.**	19	N/A	2008_Aka_2_Hugo	23/07/2008	Hugo-Anvers Trough, WAP	600	-64.807	-65.387	PQ048192	PQ043698	N/A
	A. gouldae **sp. nov.**	20	N/A	2008_Aka_4_Hugo	23/07/2008	Hugo-Anvers Trough, WAP	600	-64.807	-65.387	PQ048202	PQ043699	N/A
	A. gouldae **sp. nov.**	21	N/A	2008_Aka_5_ Lapeyrere	2/09/2008	Lapeyrere Bay, WAP	650	-64.408	-63.267	PQ048193	PQ043700	N/A
	A. gouldae **sp. nov.**	22	N/A	2008_Aka_6_ Lapeyrere	2/09/2008	Lapeyrere Bay, WAP	650	-64.408	-63.267	PQ048194	PQ043701	N/A
	A. gouldae **sp. nov.**	23	N/A	2014_Aka_1_Hugo	7/18 to 8/8/2014	Hugo-Anvers Trough, WAP	630-690	-64.841	-65.370	PQ048195	PQ043702	N/A
	A. gouldae **sp. nov.**	24	N/A	2014_Aka_2_Hugo	7/18 to 8/8/2014	Hugo-Anvers Trough, WAP	630-690	-64.841	-65.370	PQ048203	PQ043703	N/A
	A. gouldae **sp. nov.**	25	N/A	2014_Aka_3_Hugo	7/18 to 8/8/2014	Hugo-Anvers Trough, WAP	630-690	-64.841	-65.370	PQ048211	PQ043704	N/A
	A. gouldae **sp. nov.**	26	N/A	2014_Aka_4_Hugo	7/18 to 8/8/2014	Hugo-Anvers Trough, WAP	630-690	-64.841	-65.370	PQ048196	PQ043705	N/A
	A. gouldae **sp. nov.**	27	N/A	2014_Aka_5_Hugo	7/18 to 8/8/2014	Hugo-Anvers Trough, WAP	630-690	-64.841	-65.370	PQ048205	PQ043706	N/A
	A. gouldae **sp. nov.**	28	N/A	2014_Aka_6_Hugo	7/18 to 8/8/2014	Hugo-Anvers Trough, WAP	630-690	-64.841	-65.370	PQ048209	PQ043707	N/A

.....Continued on the next page

TABLE 3. (Continued)

ID	Species	Label #	Voucher ID, if any	Field ID	Collection date	Capture Location	Depth (m)	Latitude	Longitude	*mt-co1*	*mt-nd2*	*mt-cyb*
	A. gouldae **sp. nov.**	29	N/A	2014_Aka_9_Hugo	7/18 to 8/8/2014	Hugo-Anvers Trough, WAP	630-690	-64.841	-65.370	PQ048197	PQ043708	N/A
	A. gouldae **sp. nov.**	30	N/A	2014_Aka_10_Hugo	7/18 to 8/8/2014	Hugo-Anvers Trough, WAP	630-690	-64.841	-65.370	PQ048198	PQ043709	N/A
10	*A. nudiceps*	10	MNHN-2009-1057	si195n1467	31/12/2007	D'Urville Sea	839-860	-66.737	144.640	HQ712805	N/A	N/A
	A. nudiceps	31	MNHN-2009-1098	si462n3046	15/01/2008	D'Urville Sea	896	-66.404	139.794	HQ712806	N/A	N/A
	A. nudiceps	32	AN102	N/A	2020	Amundsen Sea	627	-73.520	-113.350	OK493722	N/A	N/A
	A. nudiceps	33	AN103	N/A	2020	Amundsen Sea	627	-73.520	-113.350	OK493723	N/A	N/A
	A. nudiceps	34	AN123	N/A	2020	Amundsen Sea	627	-73.520	-113.350	OK493743	N/A	N/A
	A. nudiceps	35	N/A	N/A	2012	Elephant Island, AP	N/A	N/A	N/A	NC_057664	NC_057664	NC_057664
	A. nudiceps	36	TJN 1795	AnudA	NA, pre-2003	Terra Nova bay, Ross Sea	N/A	-75.033	166.267	N/A	AY249486	N/A
	A. nudiceps	37	N/A	PS77-248-3	7/03/2011	Larsen Ice Shelf, Weddell Sea	430	-65.551	-60.197	N/A	N/A	KJ721597
	A. nudiceps	38	N/A	CHINARE-31_136	2015	Prydz Bay	103	-67.242	73.045	*	N/A	N/A
	A. nudiceps	39	N/A	CHINARE-31_137	2015	Prydz Bay	103	-67.242	73.045	*	N/A	N/A
	A. nudiceps	40	N/A	CHINARE-31_143	2015	Prydz Bay	103	-67.242	67.978	*	N/A	N/A
	A. nudiceps	41	N/A	CHINARE-31_144	2015	Prydz Bay	103	-67.242	67.978	*	N/A	N/A
	A. nudiceps	42	N/A	CHINARE-31_145	2015	Prydz Bay	103	-67.242	67.978	*	N/A	N/A
	A. nudiceps	43	N/A	CHINARE-31_146	2015	Prydz Bay	103	-67.242	65.481	*	N/A	N/A
	A. nudiceps	44	N/A	CHINARE-31_147	2015	Prydz Bay	103	-67.242	65.481	*	N/A	N/A
	A. nudiceps	45	N/A	CHINARE-31_148	2015	Prydz Bay	103	-67.242	65.481	*	N/A	N/A
	A. nudiceps	46	N/A	CHINARE-31_149	2015	Prydz Bay	103	-67.242	65.481	*	N/A	N/A
	A. nudiceps	47	N/A	CHINARE-31_150	2015	Prydz Bay	653	-69.120	65.481	*	N/A	N/A
	A. nudiceps	48	N/A	CHINARE-29_S20	2013	Prydz Bay	735	-67.999	65.481	*	N/A	N/A

the best fitting substitution model based on the corrected Akaike information criterion (AICc) (TIM3+I+G4 for all three mitochondrial markers). ML trees were constructed using the RAxML-NG web-server (Kozlov *et al.* 2019) using 50 parsimony and 50 random starting trees and a bootstrapping cutoff of 0.03.

Genetic diversity and structure

The level of genetic polymorphism was determined for each species and each locus using standard diversity indices including number of segregation sites (S), number of haplotypes (h), haplotype diversity (H_d), and nucleotide diversity (π) using the methods implemented in ARLEQUIN v.3.5.2.2 (Excoffier & Lischer 2010). Tajima's D test of selective neutrality was performed to assess deviation from the neutral model of sequence evolution. The *mt-co1* locus was used to estimate the level of genetic differentiation between the two *Akarotaxis* species through mean pairwise differences (Φ_{ST}, using the Kimura-2P model) and haplotype frequencies (F_{ST}) in ARLEQUIN v3.5.2.2 (Excoffier & Lischer 2010), using 10,000 permutations to assess significance. Genealogical relationships were estimated for each mitochondrial marker by constructing a median-joining haplotype network (Bandelt *et al.* 1999) of all available sequences of *Akarotaxis* using PopArt (Leigh & Bryant 2015).

Time calibrated phylogeny

Phylogenetic reconstruction and divergence time analyses were performed with BEAST v.2.7.1 (Bouckaert *et al.* 2019) using a partitioned dataset of concatenated *mt-co1*, *mt-nd2*, and *mt-cyb* sequences and applying a relaxed lognormal molecular clock. The dataset included all 17 bathydraconid species known to date (16 previously described species and the one described herein). Most species were represented by the three mitochondrial loci; *Psilodraco breviceps* Norman 1937 and *Bathydraco joannae* DeWitt 1985 were represented by a single marker and *Parachaenichthys georgianus* (Fischer 1885), *Vomeridens infuscipinnis* (DeWitt & Hureau 1980), *B. scotiae* Dollo 1906, and *B. antarcticus* Günther 1878 were represented by two markers. Accession numbers of the sequences used in this analysis are provided in Appendix 2.

An Optimized Relaxed Clock model was used along with a HKY+G nucleotide substitution model and a Birth-Death model of speciation. Sequences from *N. coriiceps* were included as outgroup. Time calibration of the phylogeny used two Log Normal monophyletic priors based on estimates from the most recent genome-wide time-calibrated phylogeny of notothenioids (Bista *et al.* 2023): divergence of *N. coriiceps* and bathydraconids around 7.24 MYA (2.5–97.5 inter-percentile range: 5.38–9.76 MYA) and the origin of bathydraconid group around 4.75 MYA (3.34–6.76 MYA). BEAST2 was run for 100 million MCMC iterations sampled every 10,000 generations. Convergence was assessed using Tracer v.1.7 (Rambaut *et al.* 2018) and to confirm all ESS were > 2,500. A maximum clade credibility tree with common ancestor node heights was generated using TreeAnnotator 2.7.1 and visualized with FigTree 1.4.4 (Bouckaert *et al.* 2019).

To place the time-calibrated phylogeny in a paleoclimatic context, benthic $\delta^{18}O$ (‰) data were converted to sea-surface temperature anomalies in degrees Celsius (^oC) with respect to average global temperature from 1961-1990 (Westerhold *et al.* 2020) with overlaid Loess smoothed curves of sea surface temperature evolution with a window span corresponding to 40,000 years (blue curve) and 1 million years (red curve).

Taxonomy

Akarotaxis DeWitt & Hureau 1980: 784

Type species. *Bathydraco nudiceps* Waite 1916. Davis Sea, Antarctica. By original description.

Diagnosis. A genus of Bathydraconinae (Regan 1913) with the following combination of characters: body covered with ctenoid scales; presence of two lateral lines; a small hook on the posterodorsal end of the opercle; six branchiostegal rays; small, conical teeth present; gill rakers are well-developed (Gon & Heemstra 1990).

Remarks. The genus *Akarotaxis* was erected as monotypic by DeWitt & Hureau (1980; see Sheiko 2019 for the correct date of this publication, which is frequently cited as 1979) for a species of *Bathydraco* Günther 1878 described

by Edgar R. Waite (Waite 1916) based on three specimens collected in January 1914 from a coastal area of the Davis Sea off east Antarctica (Fig. 1; Table 1). Waite and others collected these specimens while conducting benthic trawls to sample fishes of the "glacial ooze", or fine sediment deposited at the marine terminus of nearby glaciers (Waite 1916). The type specimen of *A. nudiceps* was collected at a depth of 439 m. After collecting *Bathydraco nudiceps* during an expedition to the Bellingshausen Sea off the western Antarctic Peninsula (WAP; Fig. 1; Table 1), DeWitt & Hureau (1980) noticed several major differences between *B. nudiceps* and the other members of *Bathydraco* and named the genus *Akarotaxis* for this species. Most notably, *Bathydraco* spp. possess a single lateral line, whereas *A. nudiceps* has two. In the same report, DeWitt & Hureau (1980) also described the monotypic genus *Vomeridens* (Bathydraconidae), which also possesses two lateral lines. However, the upper lateral line in *A. nudiceps* has 10 or fewer tubular scales, while *Vomeridens* possess 47–50 tubular scales.

Etymology. A combination of ακαρης (= Akaros; Greek, meaning short, or small) and ταχις (=taxis; Greek, meaning row or line) referring to the short upper lateral line (DeWitt & Hureau 1980).

***Akarotaxis gouldae* sp. nov.**
Banded Dragonfish
Figures 3–5

Akarotaxis nudiceps (Waite 1916): genetics (Near *et al.* 2012); (Bista *et al.* 2023)
Akarotaxis nudiceps (Waite 1916): early life history (Corso *et al.* 2023)

Holotype. YPM ICH 24241 (= YFTC 20826; OVERT 05053; Label #1), 140.8 mm SL, sex not determined, collected by Kuhn, K.L. and Detrich, H.W. aboard the ARSV *Laurence M. Gould* on 22 April 2010 at -64.739 S, -65.433 W.

Paratypes. YPM ICH 36536 (YFTC 20827; Label #2, 135.8 mm SL, sex unknown, collected by Kuhn, K.L. and Detrich, H.W. aboard the ARSV *Laurence M. Gould* on 22 April 2010, -64.739 S, -65.433 W); YPM ICH 20043 (YFTC 12874, Label #3, 129.3 mm SL, sex unknown, collected by Detrich, H.W. aboard the ARSV *Laurence M. Gould* on 15 May 2008, -66.266 S, -66.546 W); YPM ICH 20045 (YFTC 12876, Label #4, 127.3 mm SL, sex unknown, collected by Detrich, H.W. aboard the ARSV *Laurence M. Gould* on 15 May 2008, -66.266 S, -66.546 W); VIMS 45856 (Label #5, 136 mm SL, female, collected by Desvignes, T. aboard the ARSV *Laurence M. Gould* on 7 May 2018, -64.753 S, -65.505 W), OS 26108 (Label #6, 133 mm SL, male, collected by Desvignes, T. aboard the ARSV *Laurence M. Gould* on 20 August 2017, -64.753 S, -65.505 W); OS 26109 (Label #7, 133 mm SL, male, collected by Desvignes, T. aboard the ARSV *Laurence M. Gould* on 20 August 2017, -64.746 S, -65.481 W).

Diagnosis. A species of *Akarotaxis* distinguished from *A. nudiceps* by the presence of two dark vertical bands of pigment on the body (Figs. 3, 4); larger body depth at the origin of the anal fins (Table 2; Fig. 4); and a shorter snout and jaw length (Figs. 4, 5; Table 2).

Description. Body slender, head depressed with wide snout and elongate mouth. Dentary extends slightly past the premaxilla, with dense array of small, conical teeth on jaws (Fig. 5). Enlarged, ovoid eyes. Dorsal and anal fins high anteriorly and decrease in height posteriorly, both terminating at the beginning of the caudal region; commonly depressed in live and preserved animals (Fig. 3). Pectoral fins long, extending to anus. Caudal fin truncate. Body covered in mostly ctenoid scales; cycloid scales on the breast anterior to pelvic fins, on nape between head and dorsal fin, and on body at base of pectoral fin; no scales on head. Two lateral lines present; these are difficult to distinguish because the neuromasts are not enclosed in a canal in the scales. Both lateral lines originate near the dorsal insertion of the pectoral fin: one (the upper lateral line) ending at about the level of the seventh to tenth dorsal-fin ray (the number of non-tubular scales in this row were not counted) and the other (the middle lateral line) extending the length of the lateral flank of the body to the caudal peduncle; anteriorly the middle lateral line is partially obscured by the pectoral fin; (Fig. 3); there are 84–91 ctenoid scales on the middle lateral line (Table 2). There are 3 to 5 tubular scales at the beginning of the upper lateral line that are restricted to a position just dorsal to the shoulder girdle (ending at about the level of dorsal insertion of the pectoral fin).

Head covered in enlarged cephalic canals (see Fig. 2) with large openings in the bones covered by a thin membrane. These openings in the canals are mostly, though variably, open to the environment (i.e., represent true pores). No coronal pore present (i.e., the membrane covering the interorbital bony pore is not open to the environment). Six branchiostegal rays. Posterior end of opercle terminates in a hook shape. Morphometric data from seven *A. gouldae* **sp. nov.** type specimens summarized in Table 2. Dorsal-fin rays (D) 28–31; anal-fin rays (A)

25–28; pectoral-fin rays (P) 20–22; caudal-fin rays (C) 12–13; anterior gill rakers (GRA) (7–9) + (18–20); posterior gill rakers (GRP) (3–4) + (14–18); abdominal vertebrae 16-17; caudal vertebrae 31; total vertebrae 47-48.

Color in life. Body pale brown with two dark vertical bands that extend down the sides of the body. Band width and location varies among specimens, but one band is typically centered above the hindgut while the other is positioned above the posterior portion of the anal fin (Figs. 3, 4). Some specimens show one or two additional darker spots near the dorsal fin, but these do not extend downwards. The fleshy nostril is darkly pigmented. Caudal, pectoral fins, and opercula are generally darker than the body. Pelvic and anal fins are occasionally darker as well. Ventral surface of the abdominal region is generally lighter and more silvery than the rest of the body.

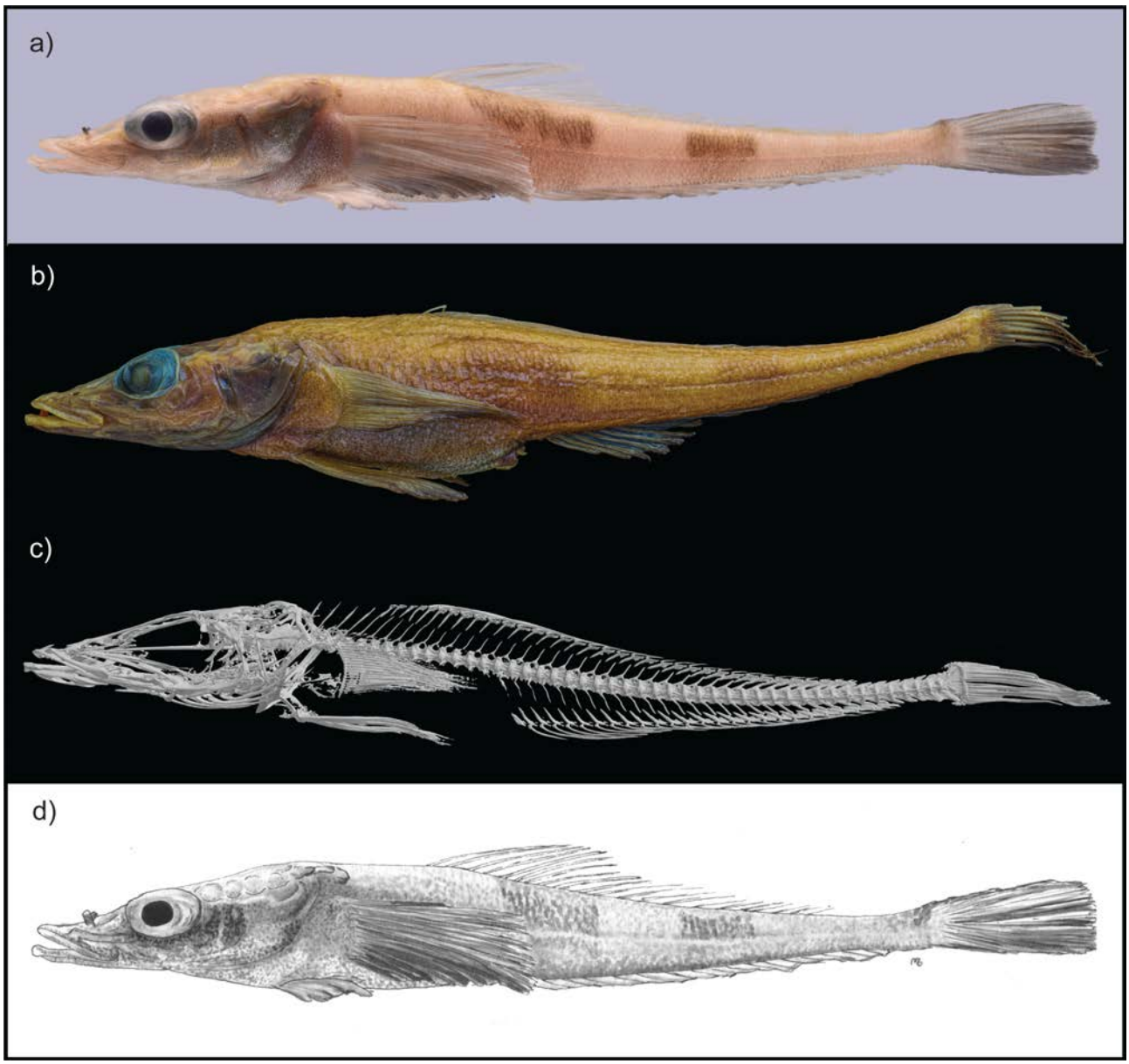

FIGURE 3. *A. gouldae* **sp. nov.** a) live specimen, collected and photographed by C.-H.C. Cheng and Elliot DeVries, off the western Antarctic Peninsula (WAP) on 08-09-2014; not preserved, b) holotype (YPM ICH 24241), c) CT scan of YPM ICH 24241 (OVERT 05053), and d) illustration by Marissa Goerke.

Color in alcohol. Body dark tan. Two vertical bands can be less apparent but still distinct. Caudal, pectoral, anal, and pelvic fins range from tan to black (Figs. 3, 4).

Remarks. Measurements for the two specimens of *A. nudiceps* presented by DeWitt & Hureau (1980) do not closely align with our data for *A. nudiceps* collected in the D'Urville Sea (Table 2). For example, the caudal length (CL), pelvic length (VL), orbital diameter (O), and head depth (HD) presented by Dewitt & Hureau (1980) are

all substantially greater than our measurements for both species (Table 2). Despite multiple attempts, we did not receive access to images or data taken directly from these specimens. However, we were able to obtain photographs of two paratypes of *A. nudiceps*, AMS IA.484 (Figs. 4h and 5h) and AMS IA.485, which lack bands and resemble the morphology described for *A. nudiceps*. These paratypes were collected January 29th, 1914 in same region as Waite's (1916) holotype. Photographs that have been presented online of freshly caught *A. nudiceps* collected in the D'urville Sea also lack bands (https://v3.boldsystems.org/index.php/Taxbrowser_Taxonpage?taxid=159627).

DeWitt & Tyler (1960) described *Akarotaxis wohlschlagi*, a junior synonym of *A. nudiceps*, based on two specimens collected in the southwestern portion of the Ross Sea. This description is the most comprehensive for the morphology of *A. nudiceps*, and it is notable that there is no suggestion of the dark bands on the body of these two specimens. We did not examine the type specimens of *A. wohlshlagi*, so we cannot comment on its synonymy with *A. goudae*. Reexamination of all *Akarotaxis* specimens, including the type specimens, should be made in the future to better distinguish between these species.

The smallest adult specimen of *A. gouldae* **sp. nov.** we examined was 127.3 mm SL (YPM ICH 20045; Fig. 4), although the sex was not determined. It is unknown when the characteristic dark vertical bands develop in *A. gouldae* **sp. nov.**, although they do not appear on larvae up to 20.7 mm SL (Corso *et al.* 2023). The presence of these bands was not reported by Waite (1916) or Dewitt & Hureau (1980) and are absent on two genetically-verified specimens of *A. nudiceps* (Fig. 6).

Etymology. *gouldae*, in honor of the U.S. Antarctic Research and Supply Vessel (*ARSV*) *Laurence M. Gould (LMG)*; for several decades this vessel has supported Antarctic Science and exploration, including the collection of the holotype and all known paratypes. The name is thus not connected to the Antarctic explorer Laurence M. Gould after which the *ARSV LMG* was named. Noun; feminine, following maritime tradition of referring to ships as female.

FIGURE 4. Images of preserved *A. gouldae* **sp. nov.** [a) YPM ICH 20043, b) YPM ICH 20045, c) YPM ICH 24241, and d) YPM ICH 36536] and *Akarotaxis nudiceps* [e) MNHN 2009-1057, f) MNHN 2009-1074, g) MNHN 2009-1075, and h) AMS IA.484]. All scale bars are 1 cm.

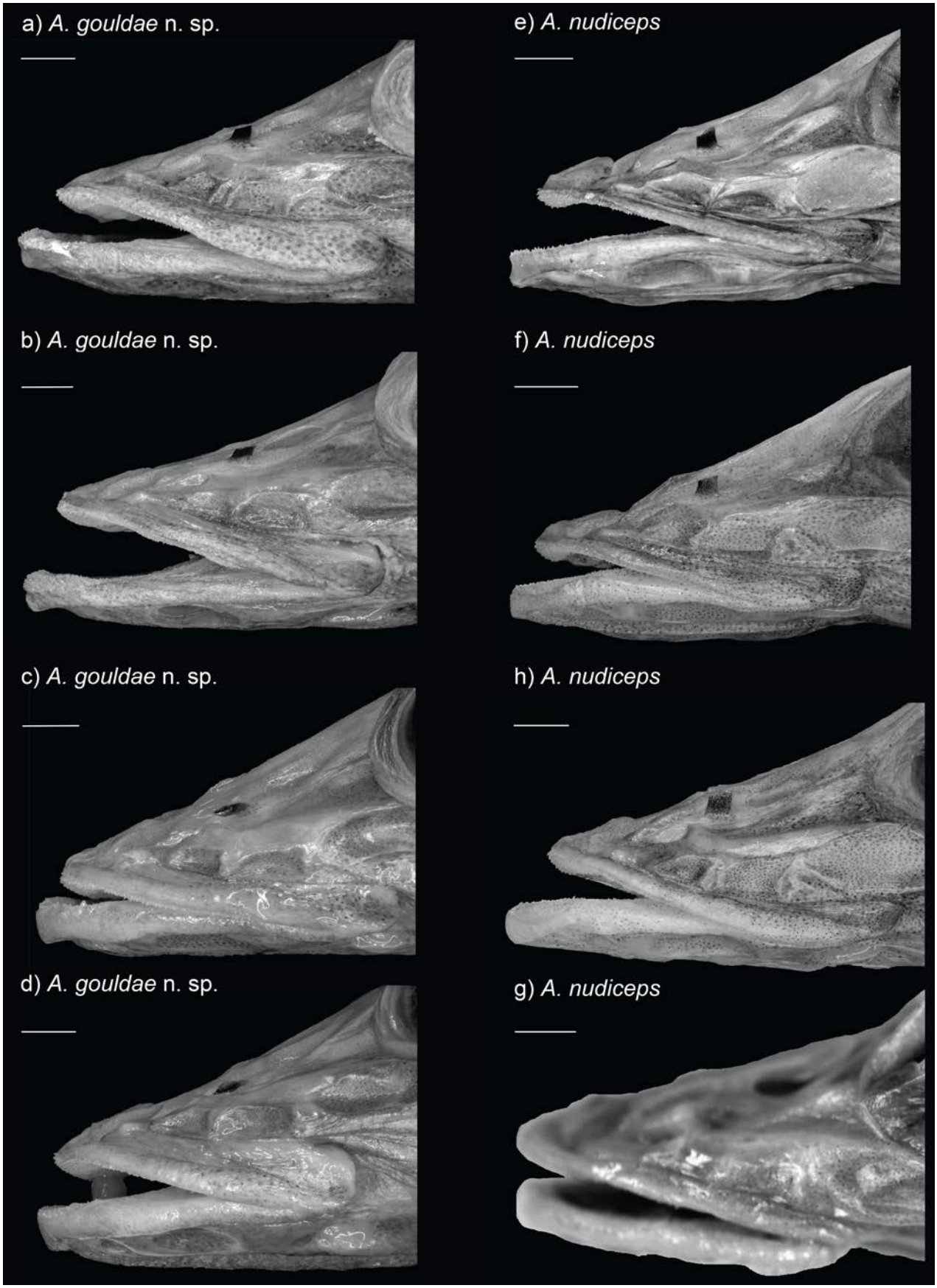

FIGURE 5. Snout comparison of *A. gouldae* **sp. nov.** [a) YPM ICH 20043, b) YPM ICH 20045, c) YPM ICH 24241, and d) YPM ICH 36536] and *Akarotaxis nudiceps* [e) MNHN 2009-1057, f) MNHN 2009-1074, g) MNHN 2009-1075, and h) AMS IA.484]. All scale bars are 2 mm, color images were converted to grayscale in order to highlight morphology.

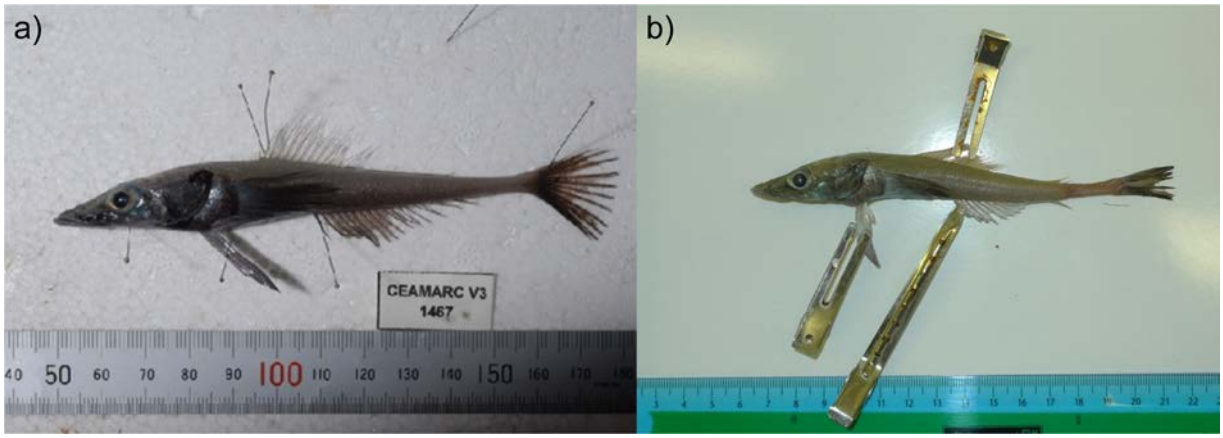

FIGURE 6. Photographs of two fresh specimens that were genetically verified as *A. nudiceps* a) MNHN-2009-1057, Label #10 (Tables 1–3) and b) PS77-248-3, Label #37 (Table 3), taken by Michael Matschiner. Note the absence of dark bands on both specimens.

Habitat, Genetics, Biogeography, and Speciation

Habitat and biology

Akarotaxis nudiceps and *A. gouldae* **sp. nov.** display similar bathymetric distributions. The depth of capture of *A. gouldae* **sp. nov.** ranged from 600 to 705 m for adults and from 215 to 964 m for larvae (Tables 1, 3) (Corso *et al.* 2023). As adults, *A. nudiceps* has been found at depths ranging from 103 to 1191 m (Eastman 2017; Li *et al.* 2022). Habitats at these depths in coastal regions of Antarctica are likely composed of similar fine sediments, as noted by Waite (1916). The difference in jaw length between species (see Table 2; Fig. 5) suggests that trophic mode may differ (Kopf *et al.* 2021). However, given probable habitat similarities *Akarotaxis* spp. would likely encounter similar prey types, especially as most smaller, deep-dwelling bathydraconids possess generalist "sit-and-wait" feeding strategies (La Mesa *et al.* 2004, 2007b; Münster *et al.* 2017). An analysis of gut contents of *Akarotaxis* spp. is necessary to further examine this hypothesis.

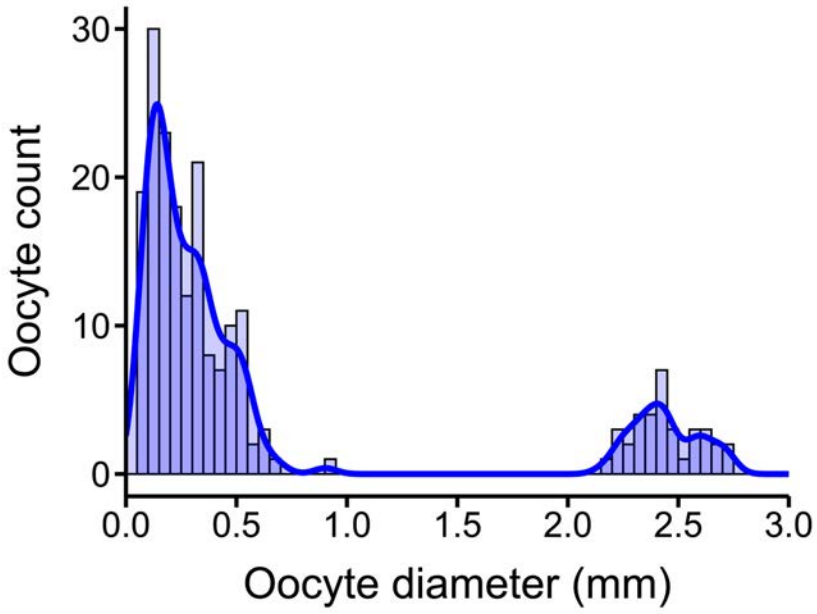

FIGURE 7. Oocyte (egg) diameter of one gravid *A. gouldae* **sp. nov.** (Aka_17_6, uncatalogued, SL = 153 mm).

We estimated that the absolute fecundity of the gravid female we examined was approximately 322 eggs (35 maturing oocytes in the ovarian fragment representing ~11% of the complete ovary weight). The bimodal size-frequency distribution of oocyte diameters aligns with observations in other bathydraconids, suggesting ovaries follow group synchronous development with likely a single spawning event (Fig. 7) (La Mesa *et al.* 2007a, 2018, 2021). The distribution of larger oocytes averaged 2.44 ± 0.15 mm (Fig. 7), which indicates the fish was preparing to spawn based on egg size of *A. nudiceps* (1.6–2.6 mm) (La Mesa *et al.* 2007a). The low fecundity of *A. gouldae* **sp. nov.** and high reproductive investment (Gonadosomatic Index of the maturing female GSI = 17%) may suggest a nesting behavior, similarly to what was proposed for *A. nudiceps* and has been observed in other bathydraconids (Barrera-Oro & Lagger 2010; Evans *et al.* 2005; La Mesa *et al.* 2007a, 2021).

Bathydraconidae phylogeny and placement of Akarotaxis spp.

We produced and/or retrieved sequences for 23 specimens of *A. gouldae* **sp. nov.** and 19 specimens of *A. nudiceps* (Table 3), including 22 *mt-nd2*, 22 *mt-co1*, four *mt-cyb* of *A. gouldae* **sp. nov.** and one *mt-nd2*, 16 *mt-co1*, one *mt-cyb*, and one complete *mt* genome sequence of *Akarotaxis nudiceps* (Table 3). In addition, we included single *mt-nd2* and *mt-co1* sequences from 13 other bathydraconid species and single *mt-cyb* sequences from 11 other bathydraconid species (see Fig. 8; Appendix 2).

Our phylogenetic analyses recovered *A. gouldae* **sp. nov.** and *A. nudiceps* as sister species with ML bootstrap support values of 100 for *mt-nd2* and *mt-cyb* for both species, and of 97 and 88 for *mt-co1* for *A. gouldae* **sp. nov.** and *A. nudiceps*, respectively (Figs. 8a, 8b, 8c). Corrected average pairwise difference Φ_{ST} and pairwise F_{ST} based on *mt-co1* confirms a significant difference between the two species ($\Phi_{ST} = 0.155$, p = <0.001; $F_{ST} = 0.157$, p = <0.001). Further, the sister species haplogroups were separated by many mutational steps: 17 for *mt-co1*, 29 for *mt-cyb*, and 43 for *mt-nd2* (Figs. 8d, 8e, 8f). Our analyses further supports the monophyly of *Akarotaxis* with ML bootstrap support of 56, 82, and 91 for *mt-co1*, *mt-nd2*, and *mt-cyb*, respectively (Figs. 8a, 8b, 8c).

Akarotaxis is resolved as the sister genus to *Bathydraco,* with a posterior probability of 1 in the three-marker time-calibrated phylogeny (Fig. 9). *Akarotaxis* and *Bathydraco* form Bathydraconinae, along with the monotypic genera *Racovitzia* (Dollo 1900), *Prionodraco* (Regan 1914)*,* and *Vomeridens* (DeWitt & Hureau 1980). While the two other dragonfish sub-families Gymnodraconinae and Cygnodraconinae were also unambiguously resolved as monophyletic with posterior probabilities of 1, the position of the Bathydraconinae as sister to Gymnodraconinae and Cygnodraconinae is supported with a posterior probability of only 0.83 (Fig. 9).

Biogeography of Akarotaxis spp.

Depending on the identity of the Dewitt and Hureau (1980) specimen, *A. nudiceps* and *A. gouldae* **sp. nov.** may have allopatric distributions or parapatric distributions with small overlaps. All adult specimens of *A. gouldae* **sp. nov.** examined in the present study and the larvae described in Corso *et al.* (2023) were captured along a ~400 km coastal section of the WAP between Lapeyrere Bay in the North and Adelaide Island in the South (Fig. 1). In contrast, *A. nudiceps* appears to possess a near circumpolar distribution in high-Antarctic coastal areas (Duhamel *et al.* 2014; Gon & Heemstra 1990). Only one specimen of *A. nudiceps* has been recorded in the coastal WAP region (DeWitt & Hureau 1980) and was used to describe the genus. This specimen, however, could not be examined here, and it is possible that it is a member of *A. gouldae* **sp. nov.** based on its capture location (Label #9 in Fig. 1).

Timing and mode of speciation

H_d and π were comparable between species (Appendix 3), with *mt-co1* H_d values of 0.79 for *A. gouldae* **sp. nov.** and 0.90 in *A. nudiceps* and *mt-co1* π values of 0.0021 for *A. gouldae* **sp. nov.** and 0.0029 in *A. nudiceps*. The star-like topology of the *mt-co1* haplotype network for *A. gouldae* **sp. nov.** (Fig. 8d) and significant Tajima's D test for neutrality (D = -2.05915, p = 0.0071, Appendix 3), suggests past contraction-expansion processes, such as population expansion following a genetic bottleneck due to drastic reductions in population size (Hewitt 2004; Provan & Bennett 2008;

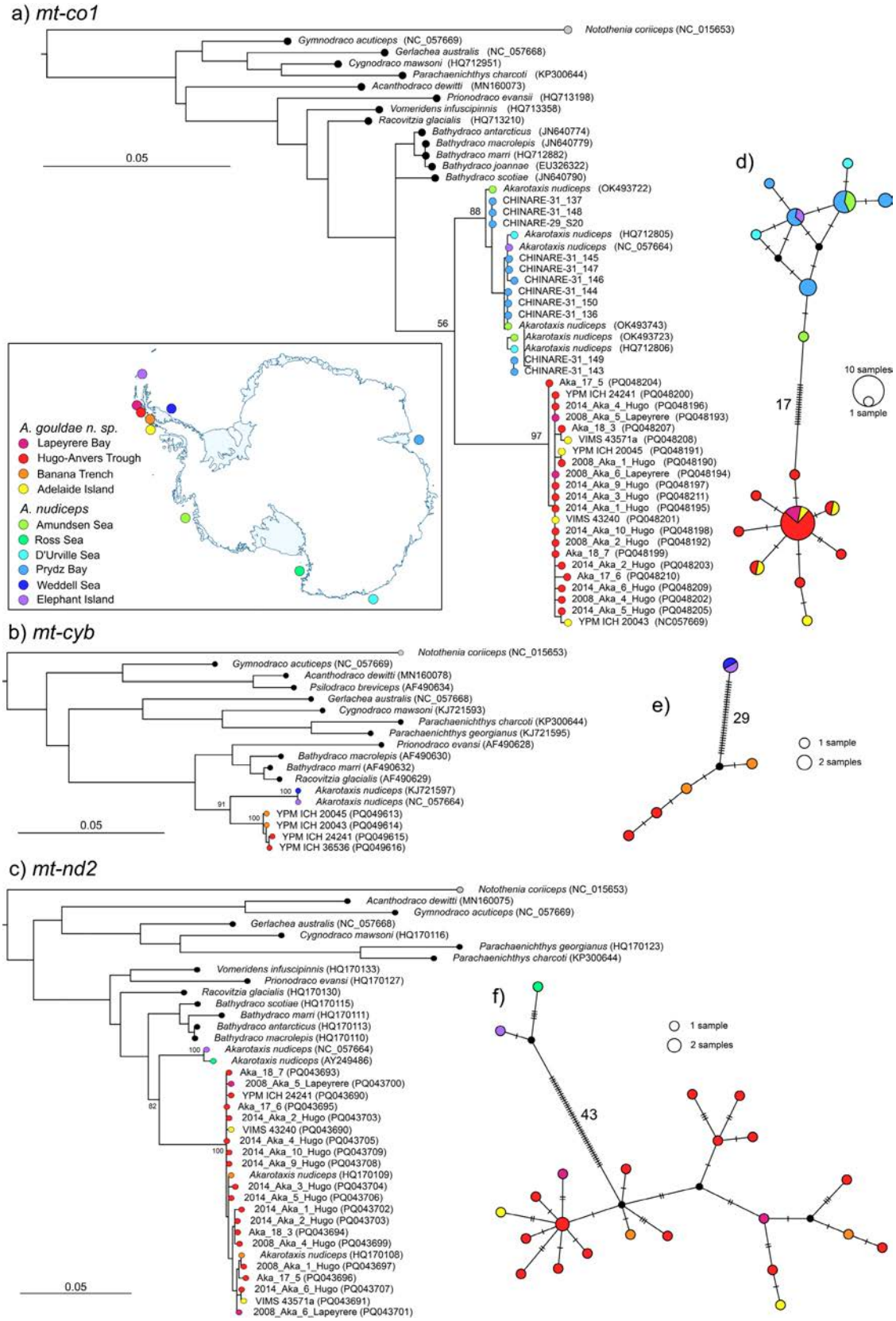

FIGURE 8. Maximum likelihood-estimated phylogenetic trees (a-c) and haplotype networks (d-f) for mitochondrial genes used in this study—*mt-co1* (a, d), *mt-cyb*, (b, e), and *mt-nd2* (c, f). Circles corresponding to *Akarotaxis* spp. in the trees are colored to match the haplotype diagrams and distribution map (inset). Scales bars for trees indicate substitution rate and scale circles for haplotype networks indicate effectives for each haplotype. Each bar on branches of the haplotype networks represents one nucleotide change. For ease of reading, the number of nucleotide changes between *A. gouldae* **sp. nov.** and *A. nudiceps* respective networks is given.

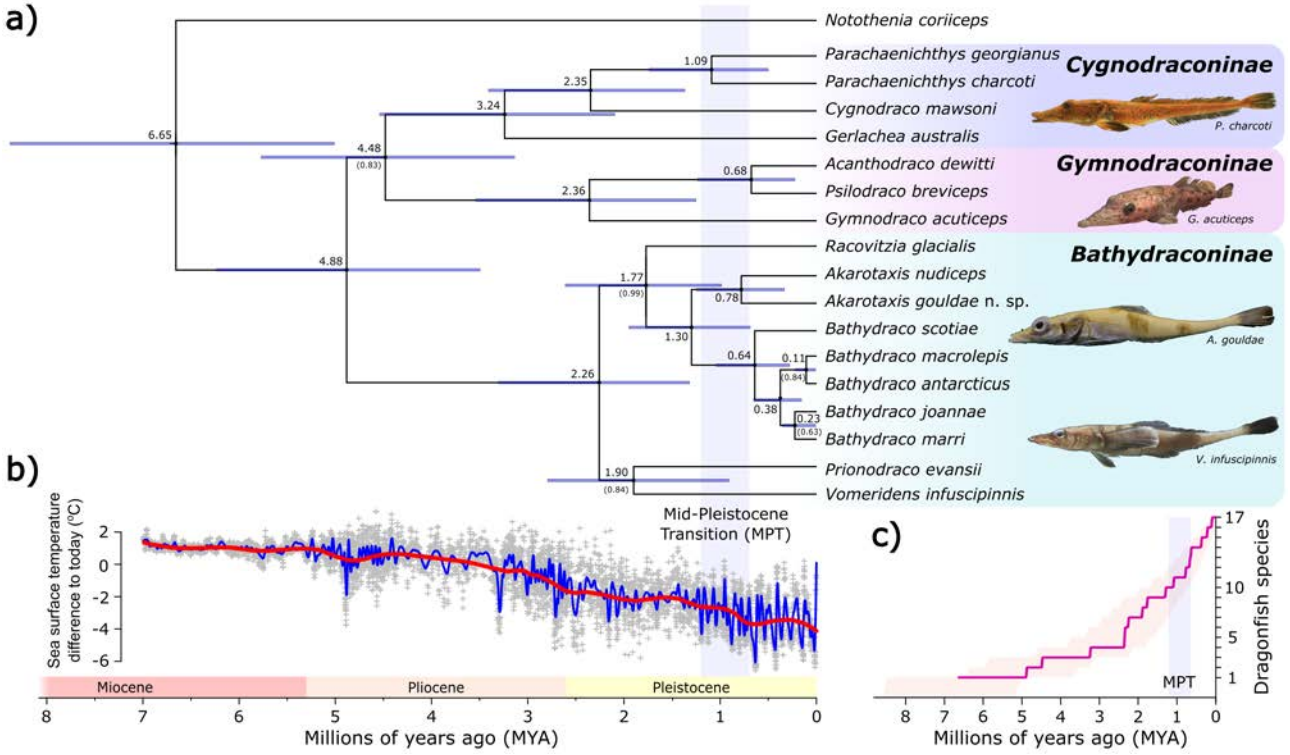

FIGURE 9. a) Time-calibrated phylogeny of Bathydraconidae based on three markers (*mt-nd2, mt-co1,* and *mt-cyb*). Divergence-time estimates are labeled at each node, with blue shading representing the 95% highest posterior density interval (HPD). All posterior probabilities were equal to 1 except when mentioned in parentheses. b) Sea surface temperature anomalies with respect to average global temperature from 1961-1990 following (Westerhold *et al*. 2020). Loess smoothed curves are overlaid with a window span corresponding to 40,000 years (blue) and 1 million years (red) and the Mid-Pleistocene Transition (MPT) highlighted in blue. c) Lineage-through-time plot for Bathydraconidae based on the time-calibrated phylogeny, with orange shading corresponding to 95% confidence interval and the Mid-Pleistocene Transition (MPT) highlighted in blue.

Marko *et al.* 2010; Maturana *et al.* 2022). While no population structure was observed in either *Akarotaxis* spp., the reticulated genealogy of the *A. nudiceps mt-co1* haplotype network (Fig. 8d) suggests that the population has not undergone a recent bottleneck. Consistently, Tajima's D test for neutrality was not significant for *A. nudiceps* (D = -0.32219, p = 0.4145, Appendix 3) suggesting that *A. nudiceps* populations evolve neutrally with no evidence of selection.

The disruptive and relatively rapid expansion of ice sheets during intermediate to maximum glacial states drove speciation among notothenioids by isolating populations in sub-Antarctic island refugia (Daane & Detrich 2022; Dornburg *et al.* 2017). Our age estimate of *A. gouldae* **sp. nov.**, at approximately 0.78 MYA (95% highest posterior density interval (HPD): 0.33–1.25 MYA) (Fig. 9a), occurs during an especially volatile period of glacial growth and collapse in West Antarctica (Collins *et al.* 2020; Pollard & DeConto 2009). The Mid-Pleistocene Transition (MPT), from 1.2 to 0.7 Mya (Fig. 9b, 9c), was characterized by a shift in Earth's climate cycles, changing from a periodicity of ~41 Kyr to 100 Kyr (Elderfield *et al.* 2012; Sutter *et al.* 2019). The warm, super-interglacial period, Marine Isotope Stage (MIS) 25 around 0.9 MYA was followed by the first 80–120 Kyr period of unperturbed Antarctic Ice Sheet growth (Sutter *et al.* 2019). Ice advances and retreats may have isolated *Akarotaxis* populations leading to the divergence of the two sister species by allopatric speciation.

Based on our time calibrated molecular phylogeny, which is the first to date to include all known Bathydraconidae, several lineages diversified during or immediately following the MPT (Fig. 9). The congeneric species *Parachaenichthys charcoti* (Vaillant 1906) on the WAP and *P. georgianus*, also from South Georgia, diverged around 1.1 MYA (95% HPD: 0.50–1.74 MYA), and the sister species *Acanthodraco dewitti* (Skóra 1995) in Antarctica and *Psilodraco breviceps*, also from South Georgia, diverged around 0.7 MYA (95% HPD: 0.23–1.24 MYA). Both sister-species pairs thus fit the model of sub-Antarctic island refugia as a source of species diversity.

In contrast, the diversification within Antarctic waters of *Akarotaxis* and *Bathydraco* around 0.65 MYA (95% HPD: 0.28–1.0 MYA), suggests a mechanism of diversification during past glacial maxima differing from the sub-Antarctic island refugia hypothesis. The apparent isolation of *A. gouldae* **sp. nov.** in deep areas of the WAP and *Akarotaxis* and *Bathydraco* being the two deepest-dwelling bathydraconid genera (Eastman 2017), supports instead the in-shelf refugium hypothesis for these species (Barnes & Kuklinski 2010; Clarke & Crame 2010; Dornburg *et al.* 2016). In this scenario, an ancestral species of *Akarotaxis* was able to survive ice progression following MIS25 through an isolated population localized in deep areas (e.g., canyons) off the WAP which diverged from the other almost circumpolar population. Based on the current range, it is unclear why *A. gouldae* **sp. nov.** was unable to expand to a wider range outside the WAP region and did not interbreed with *A. nudiceps* during subsequent interglacial periods (Barnes & Hillenbrand 2010; Marino *et al.* 2013).

Policy Implications

Based on known occurrences, *A. gouldae* **sp. nov.** has one of the most limited distributions of fishes endemic to the Southern Ocean (Duhamel *et al.* 2014). Adults and larvae have all been captured in the coastal WAP area, which is located within the Commission for the Conservation of Antarctic Marine Living Resources (CCAMLR) Subarea 48.1 (Fig. 1; CCAMLR 2017). This region, especially near the Bransfield Strait, is historically one of the regions that is most heavily targeted by the international fishery for Antarctic Krill (*Euphausia superba* Dana 1850), which is managed by CCAMLR (CCAMLR Secretariat 2022; Meyer *et al.* 2020). Fishing vessels capture krill in the epipelagic zone (0–250m) by using either midwater trawls, beam trawls, or a continuous method that pumps the net contents directly onto the ship (CCAMLR 2021). Although fishing effort was historically the greatest during austral summer (December–February), vessels have recently been fishing later into the austral autumn (March–May) to target more lipid-rich krill (CCAMLR Secretariat 2022; Meyer *et al.* 2020). Over the last five years (2017–2021), vessels averaged an aggregate annual harvest of 154, 972 tons of krill (CCAMLR Secretariat 2022).

Although there are efforts towards ecosystem-based management of Antarctic krill by CCAMLR, many current and proposed restrictions are focused on reducing the direct impact of the fishery on seabirds, adult finfishes, and marine mammals (Brooks *et al.* 2016, 2022; Meyer *et al.* 2020; Nicol & Foster 2016; Trathan *et al.* 2022; Watters *et al.* 2020). In contrast, the potential impacts of the fishery on the early life stages of Antarctic finfishes are poorly understood. In 2005, observation of the bycatch of juvenile fishes was identified as a research priority by the CCAMLR Scientific Committee (SC) (Sabourenkov & Appleyard 2005). Over a decade later, the CCAMLR SC continues to emphasize the difficulties in correctly identifying larval and juvenile finfish bycatch based on morphology (SC CAMLR 2018), while the costs of genetic methods of species identification (e.g., DNA barcoding) prevent their widespread use by monitors.

The potential endemism of *A. gouldae* **sp. nov.** to Subarea 48.1 (Fig. 1), its low fecundity, and the presence of early life stages in the epipelagic zone suggests that this species could be impacted by the krill fishery. Although bathydraconid larvae are not listed as one of the frequently captured groups of finfish bycatch (CCAMLR Secretariat 2015), the early larval stages can easily be confused with other listed nototheniids. Corso *et al.* (2023) found *A. gouldae* **sp. nov.** larvae from January–February, with several occurring near Marguerite Bay. We suggest that the exceptionally high prevalence of larval *A. gouldae* **sp. nov.** and other notothenioid larvae during the austral summer near the coastal WAP region be considered as CCAMLR continues to develop seasonal and regional closures for the krill fishery. It is critical that this vulnerable assemblage of unique fishes is protected from threats of bycatch as they are increasingly impacted by climate change (Corso *et al.* 2022; Mintenbeck *et al.* 2012).

Conclusions

The study of museum-archived *A. nudiceps* larvae by Corso *et al.* (2023) led to the discovery of *A. gouldae* **sp. nov.**, highlighting the importance of studying the early life stages of fishes to reach a comprehensive understanding of biodiversity. These combined efforts also demonstrate the continued importance of long-term ecological research (Ducklow *et al.* 2022) and of natural history collections (Hilton *et al.* 2021). Repeated annual sampling, such as that performed by the Palmer LTER, increases the likelihood of encountering rare organisms. Further, publicly

accessible repositories that care for vouchered specimens and data allow researchers to study these organisms in perpetuity, and are particularly important for coordinated efforts to studying the unique ecology of Antarctica (O'Brien *et al.* 2022). With these structures in place, our understanding of Antarctic ichthyofaunal diversity will undoubtedly continue to expand.

Acknowledgements

We thank Marissa Goerke for the illustration of *A. gouldae* **sp. nov.**, Sarah K. Huber, Gregory Watkins-Colwell, Peter Konstantinidis, Zouhaira Gabsi, Amanda Hay, Kerryn Parkinson, and Agnès Dettaï for access to specimens and curatorial assistance, Mario La Mesa, Christopher Jones, Adena Schonfeld, Joseph Cope, John H. Postlethwait, and Kharis Schrage for discussions, Amanda Hay and Kerryn Parkinson for images and x-rays of the paratype specimens of *A. nudiceps* in the AMS, William H. Detrich III and Kristen Kuhn for collection information, Michael Matschiner and Elliot DeVries for photographs and collection information, Katherine R. Murphy and Kevin Bilyk for discussion, Hai Li for gene sequences from Prydz Bay, and Stéphane Thanassekos for geographic information. We thank the captains, crew, and support staff of the R/V *Polar Duke* and ASRV *Laurence M. Gould*, the support of personnel at Palmer Station, Antarctica, and the Antarctic Support Contractors. This work was funded by the National Science Foundation Office of Polar Programs (OPP-1440435, 2026045, 1543383, 0636696, and 1142158) for specimen and environmental data collection and OPP-1947040, OPP-2232891, and Division of Biological Infrastructure (DBI-1349327) for specimen preservation and analysis, the Explorers Club, and the VIMS John Olney Fellowship.

Data availability

This paper and the nomenclatural act it contains has been registered in Zoobank (www.zoobank.org), the official register of the International Commission on Zoological Nomenclature. The LSID (Life Science Identifier) numbers are zoobank.org:pub:73F1C13C-D43B-4DCC-9E05-EB9A5B59A776 for the publication and zoobank.org:act:9CB0EA46-40B5-4E92-AB3B-F6E28277973E for *A. gouldae* **sp. nov.** Tissue samples were deposited in the Ocean Genome Legacy (OGL) Genomic Resource Collection under the Globally Unique Identifiers (GUIDs) OGL:Genomic:40297 (https://arctos.database.museum/guid/OGL:Genomic:40297) and OGL:Genomic:40275 (https://arctos.database.museum/guid/OGL:Genomic:40275) for Aka_18_003 and Aka_18_007, respectively (Falco *et al.* 2022). Edited and assembled sequence data were deposited in GenBank (https://www.ncbi.nlm.nih.gov/genbank/), corresponding to accession numbers: PQ048190 - PQ048211 (*mt-co1*); PQ043690 - PQ043709 (*mt-nd2*); and PQ049613 - PQ049616 (*mt-cyb*), see Table 3 for additional detail. Photographs, model tests, and other metadata were deposited in the United States Antarctic Program Data Center (USAP-DC) and are available on the project page: https://doi.org/10.15784/601811.

Contributions

A.D. Corso initiated the project, measured and photographed specimens, performed genetic analysis, processed genetic data, prepared the manuscript and Figures. T. Desvignes assisted with project development, performed genetic analysis, processed genetic data, prepared the manuscript and Figures. J.R. McDowell, E.E., Biesack, and C.H.C. Cheng assisted with genetic analysis and data processing. D.K. Steinberg and E.J. Hilton oversaw the project and obtained funding. E.J. Hilton led morphological analysis and helped with Figures. All authors edited and developed the manuscript.

Appendices

Appendix 1. Primers used for mitochondrial DNA amplification and sequencing, including full length NADH dehydrogenase 2 (*mt-nd2*), and partial length cytochrome c oxidase I (*mt-co1*) and cytochrome b (*mt-cyb*).

Species	Label #	*mt-nd2* primers	*mt-co1* primers	*mt-cyb* primers
A. gouldae **sp. nov.**	1–4, 16, 17	GLN and ASN (Kocher *et al.* 1995)	COI_Fish F1t1/R1t1 (Ivanova *et al.* 2007)	NotCytBf, L14724t, H15915t (Matschiner *et al.* 2011)
A. gouldae **sp. nov.**	5, 13–15	GLN and ASN (Kocher *et al.* 1995)	Noto-co1-F1/R1 (Desvignes *et al.* 2019)	
A. gouldae **sp. nov.**	18-30	GLN and ASN (Kocher *et al.* 1995)	COI_Fish F1t1/R1t1 (Ivanova *et al.* 2007)	

Appendix 2. Accession numbers of additional sequences used in the phylogenetic analyses. * Sequences used for the time-calibrated phylogeny.

Species	*mt-co1*	*mt-nd2*	*mt-cyb*
Acanthodraco dewitti	MN160073	MN160075	MN160078
Bathydraco antarcticus	JN640774	HQ170113	N/A
Bathydraco joannae	EU326322	N/A	N/A
Bathydraco macrolepis	JN640779	HQ170110	AF490630
Bathydraco marri	HQ712882	HQ170111	AF490632
Bathydraco scotiae	JN640790	HQ170115	N/A
Cygnodraco mawsoni	HQ712951	HQ170116	KJ721593
Gerlachea australis	NC_057668	NC_057668	NC_057668
Gymnodraco acuticeps	NC_057669	NC_057669	NC_057669
Parachaenichthys charcoti	KP300644	KP300644	KP300644
Parachaenichthys georgianus	N/A	HQ170123	KJ721595
Prionodraco evansii	HQ713198	HQ170127	AF490628
Psilodraco breviceps	N/A	N/A	AF490634
Racovitzia glacialis	HQ713210	HQ170130	AF490629
Vomeridens infuscipinnis	HQ713358	HQ170133	N/A
Notothenia corriceps	NC_015653	NC_015653	NC_015653
Akarotaxis gouldae **sp. nov.***	PQ048200	PQ043695	PQ049613
Akarotaxis nudiceps *	NC_057664	NC_057664	NC_057664

Appendix 3. Results of the genetic polymorphism analysis. Grey cells highlight results of analyses performed for thoroughness but however unreliable due to too small sample sizes.

		Sequences #	Segregating sites	Haplotype #	Haplotype Diversity	Nucleotide Diversity	Tajima's Test	
Marker	**Species**	N	S	h	H_d	π	D	p-value
mt-co1	*A. nudiceps*	16	7	9	0.9	0.002949	-0.32219	0.4145
	A. gouldae **sp. nov.**	19	11	11	0.7895	0.002069	-2.05915	0.0071
mt-nd2	*A. nudiceps*	2	5	2	1	0.004808	0	1
	A. gouldae **sp. nov.**	22	29	21	0.9957	0.005179	-1.24154	0.0956
mt-cyb	*A. nudiceps*	2	0	1	0	0	0	1
	A. gouldae **sp. nov.**	4	4	4	1	0.002016	-0.06501	0.5894

References

Bandelt, H.J., Forster, P. & Röhl, A. (1999) Median-joining networks for inferring intraspecific phylogenies. *Molecular Biology and Evolution*, 16 (1), 37–48.
https://doi.org/10.1093/oxfordjournals.molbev.a026036

Barnes, D.K.A. & Hillenbrand, C.-D. (2010) Faunal evidence for a late quaternary trans-Antarctic seaway. *Global Change Biology*, 16 (12), 3297–3303.
https://doi.org/10.1111/j.1365-2486.2010.02198.x

Barnes, D.K.A. & Kuklinski, P. (2010) Bryozoans of the Weddell Sea continental shelf, slope and abyss: did marine life colonize the Antarctic shelf from deep water, outlying islands or in situ refugia following glaciations? *Journal of Biogeography*, 37 (9), 1648–1656.
https://doi.org/10.1111/j.1365-2699.2010.02320.x

Barrera-Oro, E.R. & Lagger, C. (2010) Egg-guarding behaviour in the Antarctic bathydraconid dragonfish *Parachaenichthys charcoti*. *Polar Biology*, 33, 1585–1587.
https://doi.org/10.1007/s00300-010-0847-3

Beck, E.A., Healey, H.M., Small, C.M., Currey, M.C., Desvignes, T., Cresko, W.A. & Postlethwait, J.H. (2022) Advancing human disease research with fish evolutionary mutant models. *Trends in Genetics*, 38 (1), 22–44.
https://doi.org/10.1016/j.tig.2021.07.002

Bilyk, K.T., Zhuang, X., Murphy, K.R. & Cheng, C.-H.C. (2019) A tale of two genes: divergent evolutionary fate of haptoglobin and hemopexin in hemoglobinless Antarctic icefishes. *Journal of Experimental Biology*, 222 (6), jeb188573.
https://doi.org/10.1242/jeb.188573

Bista, I., Wood, J.M.D., Desvignes, T., McCarthy, S.A., Matschiner, M., Ning, Z., Tracey, A., Torrance, J., Sims, Y., Chow, W., Smith, M., Oliver, K., Haggerty, L., Salzburger, W., Postlethwait, J.H., Howe, K., Clark, M.S., William Detrich, H., Christina Cheng, C.-H., Miska, E.A. & Durbin, R. (2023) Genomics of cold adaptations in the Antarctic notothenioid fish radiation. *Nature Communications*, 14, 3412.
https://doi.org/10.1038/s41467-023-38567-6

Bouckaert, R., Vaughan, T.G., Barido-Sottani, J., Duchêne, S., Fourment, M., Gavryushkina, A., Heled, J., Jones, G., Kühnert, D., Maio, N.D., Matschiner, M., Mendes, F.K., Müller, N.F., Ogilvie, H.A., Plessis, L. du, Popinga, A., Rambaut, A., Rasmussen, D., Siveroni, I., Suchard, M.A., Wu, C.-H., Xie, D., Zhang, C., Stadler, T. & Drummond, A.J. (2019) BEAST 2.5: An advanced software platform for Bayesian evolutionary analysis. *PLOS Computational Biology*, 15 (4), e1006650.
https://doi.org/10.1371/journal.pcbi.1006650

Brooks, C.M., Ainley, D.G., Jacquet, J., Chown, S.L., Pertierra, L.R., Francis, E., Rogers, A., Chavez-Molina, V., Teh, L. & Sumaila, U.R. (2022) Protect global values of the Southern Ocean ecosystem. *Science*, 378 (6619), 477–479.
https://doi.org/10.1126/science.add9480

Brooks, C.M., Crowder, L.B., Curran, L.M., Dunbar, R.B., Ainley, D.G., Dodds, K.J., Gjerde, K.M. & Sumaila, U.R. (2016) Science-based management in decline in the Southern Ocean. *Science*, 354 (6309), 185–187.
https://doi.org/10.1126/science.aah4119

Cao, S., Li, Y., Miao, X., Zhang, R., Lin, L. & Li, H. (2022) DNA barcoding provides insights into Fish Diversity and Molecular Taxonomy of the Amundsen Sea. *Conservation Genetics Resources*, 14 (3), 281–289.
https://doi.org/10.1007/s12686-022-01273-4

Commission for the Conservation of Antarctic Marine Living Resources (CCAMLR). (2017) Map of the CAMLR Convention Area. Last updated October 2017. Available from: www.ccamlr.org/node/86816 (accessed 1 December 2022)

CCAMLR. (2018) Report of the thirty-seventh meeting of the Scientific Committee. Available from: https://meetings.ccamlr.org/en/ccamlr-xxxvii/38 (accessed 1 December 2022)

CCAMLR. (2021) Krill fisheries. Last updated July 2021. Available from: https://www.ccamlr.org/en/fisheries/krill (accessed 1 December 2022)

CCAMLR Secretariat (2015) Common fish by-catch species in CCAMLR krill fisheries. Last updated March 2015. Available from: https://www.ccamlr.org/en/document/science/common-fish-catch-species-ccamlr-krill-fisheries (accessed 1 December 2022)

CCAMLR Secretariat (2022) Fishery Report 2021: *Euphausia superba* in Area 48. Available from: https://fishdocs.ccamlr.org/FishRep_48_KRI_2021.html (accessed 1 December 2022)

Ceballos, S.G., Roesti, M., Matschiner, M., Fernández, D.A., Damerau, M., Hanel, R. & Salzburger, W. (2019) Phylogenomics of an extra-Antarctic notothenioid radiation reveals a previously unrecognized lineage and diffuse species boundaries. *BMC Evolutionary Biology*, 19, 1–14.
https://doi.org/10.1186/s12862-019-1345-z

Clarke, A. & Crame, J.A. (2010) Evolutionary dynamics at high latitudes: speciation and extinction in polar marine faunas. *Philosophical Transactions of the Royal Society B: Biological Sciences*, 365 (1558), 3655–3666.
https://doi.org/10.1098/rstb.2010.0270

Collins, G.E., Hogg, I.D., Convey, P., Sancho, L.G., Cowan, D.A., Lyons, W.B., Adams, B.J., Wall, D.H. & Green, T.G.A.

(2020) Genetic diversity of soil invertebrates corroborates timing estimates for past collapses of the West Antarctic Ice Sheet. *Proceedings of the National Academy of Sciences*, 117 (36), 22293–22302.
https://doi.org/10.1073/pnas.2007925117

Corso, A.D., McDowell, J.R., Biesack, E.E., Muffelman, S.C. & Hilton, E.J. (2023) Larval stages of the Antarctic Dragonfish *Akarotaxis nudiceps* (Waite, 1916), with comments on the larvae of the morphologically similar species *Prionodraco evansii* Regan 1914 (Notothenioidei: Bathydraconidae). *Journal of Fish Biology*, 102 (2), 395–402.
https://doi.org/10.1111/jfb.15267

Corso, A.D., Steinberg, D.K., Stammerjohn, S.E. & Hilton, E.J. (2022) Climate drives long-term change in Antarctic Silverfish along the western Antarctic Peninsula. *Communications biology*, 5 (1), 1–10.
https://doi.org/10.1038/s42003-022-03042-3

Daane, J.M. & Detrich, H.W. (2022) Adaptations and Diversity of Antarctic Fishes: A Genomic Perspective. *Annual Review of Animal Biosciences*, 10, 39–62.
https://doi.org/10.1146/annurev-animal-081221-064325

Dana, J.D. (1850) Synopsis generum crustaceorum ordinis "Schizopoda." *American Journal of Science and Arts*, 9, 129–133.

Darriba, D., Posada, D., Kozlov, A.M., Stamatakis, A., Morel, B. & Flouri, T. (2020) ModelTest-NG: A New and Scalable Tool for the Selection of DNA and Protein Evolutionary Models. *Molecular Biology and Evolution*, 37 (1), 291–294.
https://doi.org/10.1093/molbev/msz189

Derome, N., Chen, W.-J., Dettaÿ, A., Bonillo, C. & Lecointre, G. (2002) Phylogeny of Antarctic dragonfishes (Bathydraconidae, Notothenioidei, Teleostei) and related families based on their anatomy and two mitochondrial genes. *Molecular Phylogenetics and Evolution*, 24 (1), 139–152.
https://doi.org/10.1016/S1055-7903(02)00223-3

Desvignes, T., Le François, N.R., Goetz, L.C., Smith, S.S., Shusdock, K.A., Parker, S.K., Postlethwait, J.H. & Detrich, H.W. (2019) Intergeneric hybrids inform reproductive isolating barriers in the Antarctic icefish radiation. *Scientific Reports*, 9 (1), 5989.
https://doi.org/10.1038/s41598-019-42354-z

Desvignes, T., Postlethwait, J.H. & Konstantinidis, P. (2020) Biogeography of the Antarctic dragonfishes *Acanthodraco dewitti* and *Psilodraco breviceps* with re-description of *Acanthodraco dewitti* larvae (Notothenioidei: Bathydraconidae). *Polar Biology*, 43 (5), 565–572.
https://doi.org/10.1007/s00300-020-02661-y

DeWitt, H.H. (1985) Reports on fishes of the university of southern California, Antarctic research program, 1962–1968. I: A review of the genus *Bathydraco* Gunther (Family Bathydraconidae). *Cybium*, 9, 295–314.

DeWitt, H.H. & Hureau, J.C. (1980) Fishes collected during" Hero" cruise 72–2 in the Palmer Archipelago, Antarctic, with the description of two new general and three new species. *Bulletin du Museum National d'Histoire Naturelle*, 3, 775–820.
https://doi.org/10.5962/p.283193

Dollo, L. (1900) *Racovitzia glacialis*, poisson abyssal nouveau, recueilli par cette expédition. Expédition Antarctique Belge. *Communication Préliminaire. Bulletins de l'Académie royale des sciences, des lettres et des beaux-arts de Belgique*, 4, 316–327.

Dollo, L. & Traquair, M.R.H. (1906) *Bathydraco Scotiæ*, Poisson abyssal nouveau recueilli par l'Expédition Antarctique Nationale Ecossaise. *Proceedings of the Royal Society of Edinburgh*, 26, 65–75.
https://doi.org/10.1017/S0370164600024433

Dornburg, A., Federman, S., Eytan, R.I. & Near, T.J. (2016) Cryptic species diversity in sub-Antarctic islands: A case study of *Lepidonotothen*. *Molecular Phylogenetics and Evolution*, 104, 32–43.
https://doi.org/10.1016/j.ympev.2016.07.013

Dornburg, A., Federman, S., Lamb, A.D., Jones, C.D. & Near, T.J. (2017) Cradles and museums of Antarctic teleost biodiversity. *Nature Ecology & Evolution*, 1 (9), 1379–1384.
https://doi.org/10.1038/s41559-017-0239-y

Dorschel, B., Hehemann, L., Viquerat, S., Warnke, F., Dreutter, S., Tenberge, Y.S., Accettella, D., An, L., Barrios, F., Bazhenova, E., Black, J., Bohoyo, F., Davey, C., De Santis, L., Dotti, C.E., Fremand, A.C., Fretwell, P.T., Gales, J.A., Gao, J., Gasperini, L., Greenbaum, J.S., Jencks, J.H., Hogan, K., Hong, J.K., Jakobsson, M., Jensen, L., Kool, J., Larin, S., Larter, R.D., Leitchenkov, G., Loubrieu, B., Mackay, K., Mayer, L., Millan, R., Morlighem, M., Navidad, F., Nitsche, F.O., Nogi, Y., Pertuisot, C., Post, A.L., Pritchard, H.D., Purser, A., Rebesco, M., Rignot, E., Roberts, J.L., Rovere, M., Ryzhov, I., Sauli, C., Schmitt, T., Silvano, A., Smith, J., Snaith, H., Tate, A.J., Tinto, K., Vandenbossche, P., Weatherall, P., Wintersteller, P., Yang, C., Zhang, T. & Arndt, J.E. (2022) The International Bathymetric Chart of the Southern Ocean Version 2. *Scientific Data*, 9 (1), 275.
https://doi.org/10.1038/s41597-022-01366-7

Ducklow, H., Cimino, M., Dunton, K.H., Fraser, W.R., Hopcroft, R.R., Ji, R., Miller, A.J., Ohman, M.D. & Sosik, H.M. (2022) Marine pelagic ecosystem responses to climate variability and change. *BioScience*, 72 (9), 827–850.
https://doi.org/10.1093/biosci/biac050

Duhamel, G., Hulley, P.-A., Causse, R., Koubbi, P., Vacchi, M., Pruvost, P., Vigetta, S., Irisson, J.O., Mormède, S. & Belchier, M., Dettai, A., Detrich, H.W., Gutt, J., Jones, C.D., Kock, K.H., Lopez Abellan, L.J. & Van de Putte, A.P. (2014) Chapter 7. Biogeographic Patterns of Fish. *In*: De Broyer, C., Koubbi, P., Griffiths, H.J., Raymond, B., d'Udekem d'Acoz, C., Van de Putte, A., Danis, B., David, B., Grant, S., Gutt, J., Held, C., Hosie, G., Huettmann, F., Post, A. & Ropert-Coudert, Y. (Eds.),

Biogeographic Atlas of the Southern Ocean. Scientific Committee on Antarctic Research, Cambridge, pp. 328–362.
Eastman, J.T. (2017) Bathymetric distributions of notothenioid fishes. *Polar Biology*, 40 (10), 2077–2095. https://doi.org/10.1007/s00300-017-2128-x
Eastman, J.T. & Eakin, R.R. (2021) Checklist of the species of notothenioid fishes. *Antarctic Science*, 33 (3), 273–280. https://doi.org/10.1017/S0954102020000632
Eastman, J.T. & McCune, A.R. (2000) Fishes on the Antarctic continental shelf: evolution of a marine species flock? *Journal of Fish Biology*, 57, 84–102. https://doi.org/10.1111/j.1095-8649.2000.tb02246.x
Edler, D., Klein, J., Antonelli, A. & Silvestro, D. (2021) raxmlGUI 2.0: A graphical interface and toolkit for phylogenetic analyses using RAxML. *Methods in Ecology and Evolution*, 12 (2), 373–377. https://doi.org/10.1111/2041-210X.13512
Ekau, W. (1990) Demersal fish fauna of the Weddell Sea, Antarctica. *Antarctic Science*, 2 (2), 129–137. https://doi.org/10.1017/S0954102090000165
Elderfield, H., Ferretti, P., Greaves, M., Crowhurst, S., McCave, I.N., Hodell, D. & Piotrowski, A.M. (2012) Evolution of Ocean Temperature and Ice Volume Through the Mid-Pleistocene Climate Transition. *Science*, 337 (6095), 704–709. https://doi.org/10.1126/science.1221294
Evans, C.W., Cziko, P., Cheng, C.-H.C. & Devries, A.L. (2005) Spawning behaviour and early development in the naked dragonfish *Gymnodraco acuticeps*. *Antarctic Science*, 17 (3), 319–327. https://doi.org/10.1017/S0954102005002749
Excoffier, L. & Lischer, H.E.L. (2010) Arlequin suite ver 3.5: a new series of programs to perform population genetics analyses under Linux and Windows. *Molecular Ecology Resources*, 10 (3), 564–567. https://doi.org/10.1111/j.1755-0998.2010.02847.x
Falco, R., Appiah-Madson, H.J. & Distel, D.L. (2022) The Ocean Genome Legacy: A Genomic Resource Repository for Marine Life. *Biopreservation and Biobanking*, 20, 104–106. https://doi.org/10.1089/bio.2021.0148
Fischer, J.G. (1885) Über Fische von Süd-Georgien. *Ichthyologische und herpetologische Bemerkungen. Jahrbuch der Hamburgischen Wissenschaftlichen Anstalten*, 2, 49–65.
Gon, O. & Heemstra, P.C. (1990) *Fishes of the Southern Ocean*. JLB Smith Institute of Ichthyology, Grahamstown, 462 pp. https://doi.org/10.5962/bhl.title.141868
Günther, A. (1878) Preliminary notices of Deep-Sea Fishes collected during the Voyage of HMS "Challenger." *Journal of Natural History*, 2 (7), 17–28. https://doi.org/10.1080/00222937808682376
Hewitt, G.M. (2004) Genetic consequences of climatic oscillations in the Quaternary. *Philosophical Transactions of the Royal Society of London. Series B: Biological Sciences*, 359 (1442), 183–195. https://doi.org/10.1098/rstb.2003.1388
Hilton, E.J., Watkins-Colwell, G.J. & Huber, S.K. (2021) The Expanding Role of Natural History Collections. *Ichthyology & Herpetology*, 109 (2), 379–391. https://doi.org/10.1643/t2020018
Ivanova, N.V., Zemlak, T.S., Hanner, R.H. & Hebert, P.D. (2007) Universal primer cocktails for fish DNA barcoding. *Molecular Ecology Notes*, 7 (4), 544–548. https://doi.org/10.1111/j.1471-8286.2007.01748.x
Katoh, K., Rozewicki, J. & Yamada, K.D. (2019) MAFFT online service: multiple sequence alignment, interactive sequence choice and visualization. *Briefings in Bioinformatics*, 20 (4), 1160–1166. https://doi.org/10.1093/bib/bbx108
Kocher, T.D., Conroy, J.A., McKaye, K.R., Stauffer, J.R. & Lockwood, S.F. (1995) Evolution of NADH Dehydrogenase Subunit 2 in East African Cichlid Fish. *Molecular Phylogenetics and Evolution*, 4 (4), 420–432. https://doi.org/10.1006/mpev.1995.1039
Kopf, R.K., Yen, J.D.L., Nimmo, D.G., Brosse, S. & Villéger, S. (2021) Global patterns and predictors of trophic position, body size and jaw size in fishes. *Global Ecology and Biogeography*, 30 (2), 414–428. https://doi.org/10.1111/geb.13227
Kozlov, A.M., Darriba, D., Flouri, T., Morel, B. & Stamatakis, A. (2019) RAxML-NG: a fast, scalable and user-friendly tool for maximum likelihood phylogenetic inference. *Bioinformatics*, 35 (21), 4453–4455. https://doi.org/10.1093/bioinformatics/btz305
Kuhn, K.L., Near, T.J., Detrich, H.W. & Eastman, J.T. (2011) Biology of the Antarctic dragonfish *Vomeridens infuscipinnis* (Notothenioidei: Bathydraconidae). *Antarctic Science*, 23 (1), 18–26. https://doi.org/10.1017/S095410201000060X
La Mesa, M., Calì, F., Donato, F., Riginella, E. & Mazzoldi, C. (2018) Aspects of the biology of the Antarctic dragonfish *Gerlachea australis* (Notothenioidei: Bathydraconidae) in the Weddell Sea, Antarctica. *Polar Biology*, 41, 793–803. https://doi.org/10.1007/s00300-017-2240-y
La Mesa, M., Caputo, V. & Eastman, J.T. (2007a) Gametogenesis in the dragonfishes *Akarotaxis nudiceps* and *Bathydraco marri* (Pisces, Notothenioidei: Bathydraconidae) from the Ross Sea. *Antarctic Science*, 19 (1), 64–70. https://doi.org/10.1017/S0954102007000090

La Mesa, M., Eastman, J.T. & Licandro, P. (2007b) Feeding habits of *Bathydraco marri* (Pisces, Notothenioidei, Bathydraconidae) from the Ross Sea, Antarctica. *Polar Biology*, 30, 541–547.
https://doi.org/10.1007/s00300-006-0211-9
La Mesa, M., Eastman, J.T. & Vacchi, M. (2004) The role of notothenioid fish in the food web of the Ross Sea shelf waters: a review. *Polar Biology*, 27, 321–338.
https://doi.org/10.1007/s00300-004-0599-z
La Mesa, M., Llompart, F., Riginella, E. & Eastman, J.T. (2021) Parental care and reproductive strategies in notothenioid fishes. *Fish and Fisheries*, 22 (2), 356–376.
https://doi.org/10.1111/faf.12523
La Mesa, M., Piepenburg, D., Pineda-Metz, S.E.A., Riginella, E. & Eastman, J.T. (2019) Spatial distribution and habitat preferences of demersal fish assemblages in the southeastern Weddell Sea (Southern Ocean). *Polar Biology*, 42, 1025–1040.
https://doi.org/10.1007/s00300-019-02495-3
Lecointre, G., Améziane, N., Boisselier, M.-C., Bonillo, C., Busson, F., Causse, R., Chenuil, A., Couloux, A., Coutanceau, J.-P. & Cruaud, C. (2013) Is the species flock concept operational? The Antarctic shelf case. *PloS one*, 8 (8), e68787.
https://doi.org/10.1371/journal.pone.0068787
Leigh, J.W. & Bryant, D. (2015) popart: full-feature software for haplotype network construction. *Methods in Ecology and Evolution*, 6 (9), 1110–1116.
https://doi.org/10.1111/2041-210X.12410
Li, H., Cao, S., Li, Y., Song, P., Zhang, R., Wang, R., Liu, S., Miao, X. & Lin, L. (2022) Molecular assessment of demersal fish diversity in Prydz Bay using DNA taxonomy. *Deep Sea Research Part II: Topical Studies in Oceanography*, 202, 105140.
https://doi.org/10.1016/j.dsr2.2022.105140
Lönnberg, E. (1906) *Contributions to the fauna of South Georgia*. Almqvist & Wiksells, Uppsala, 104 pp.
Marino, I. a. M., Benazzo, A., Agostini, C., Mezzavilla, M., Hoban, S.M., Patarnello, T., Zane, L. & Bertorelle, G. (2013) Evidence for past and present hybridization in three Antarctic icefish species provides new perspectives on an evolutionary radiation. *Molecular Ecology*, 22 (20), 5148–5161.
https://doi.org/10.1111/mec.12458
Marko, P.B., Hoffman, J.M., Emme, S.A., Mcgovern, T.M., Keever, C.C. & Nicole Cox, L. (2010) The "Expansion–Contraction" model of Pleistocene biogeography: rocky shores suffer a sea change? *Molecular Ecology*, 19 (1), 146–169.
https://doi.org/10.1111/j.1365-294X.2009.04417.x
Matschiner, M., Hanel, R. & Salzburger, W. (2011) On the origin and trigger of the notothenioid adaptive radiation. *PLoS one*, 6 (4), e18911.
https://doi.org/10.1371/journal.pone.0018911
Maturana, C.S., Biersma, E.M., Díaz, A., González-Wevar, C., Contador, T., Convey, P., Jackson, J.A. & Poulin, E. (2022) Survivors and colonizers: Contrasting biogeographic histories reconciled in the Antarctic freshwater copepod *Boeckella poppei*. *Frontiers in Ecology and Evolution*, 10, 1012852.
https://doi.org/10.3389/fevo.2022.1012852
La Mesa, M., Riginella, E. & Jones, C.D. (2017) Early life history traits and geographical distribution of *Parachaenichthys charcoti. Antarctic Science*, 29 (5), 410–416.
https://doi.org/10.1017/S0954102017000189
Meyer, B., Atkinson, A., Bernard, K.S., Brierley, A.S., Driscoll, R., Hill, S.L., Marschoff, E., Maschette, D., Perry, F.A., Reiss, C.S., Rombolá, E., Tarling, G.A., Thorpe, S.E., Trathan, P.N., Zhu, G. & Kawaguchi, S. (2020) Successful ecosystem-based management of Antarctic krill should address uncertainties in krill recruitment, behaviour and ecological adaptation. *Communications Earth & Environment*, 1 (1), 1–12.
https://doi.org/10.1038/s43247-020-00026-1
Miller, R.G. (1993) *History and atlas of the fishes of the Antarctic Ocean.* Foresta Institute for Ocean and Mountain Studies, Carson City, 792 pp.
Mintenbeck, K., Barrera-Oro, E.R., Brey, T., Jacob, U., Knust, R., Mark, F.C., Moreira, E., Strobel, A. & Arntz, W.E. (2012) Impact of climate change on fishes in complex Antarctic ecosystems. *Advances in ecological research*, 351–426.
https://doi.org/10.1016/B978-0-12-396992-7.00006-X
Münster, J., Kochmann, J., Grigat, J., Klimpel, S. & Kuhn, T. (2017) Parasite fauna of the Antarctic dragonfish *Parachaenichthys charcoti* (Perciformes: Bathydraconidae) and closely related Bathydraconidae from the Antarctic Peninsula, Southern Ocean. *Parasites & Vectors*, 10, 1–9.
https://doi.org/10.1186/s13071-017-2176-7
Near, T.J., Dornburg, A., Kuhn, K.L., Eastman, J.T., Pennington, J.N., Patarnello, T., Zane, L., Fernández, D.A. & Jones, C.D. (2012) Ancient climate change, antifreeze, and the evolutionary diversification of Antarctic fishes. *Proceedings of the National Academy of Sciences*, 109 (9), 3434–3439.
https://doi.org/10.1073/pnas.1115169109
Near, T.J., MacGuigan, D.J., Parker, E., Struthers, C.D., Jones, C.D. & Dornburg, A. (2018) Phylogenetic analysis of Antarctic notothenioids illuminates the utility of RADseq for resolving Cenozoic adaptive radiations. *Molecular Phylogenetics and Evolution*, 129, 268–279.

https://doi.org/10.1016/j.ympev.2018.09.001
Nicol, S. & Foster, J. (2016) The Fishery for Antarctic Krill: Its Current Status and Management Regime. *In*: Siegel, V. (Ed.), *Biology and Ecology of Antarctic Krill*. *Advances in Polar Ecology*. Springer International Publishing, Cham, pp. 387–421.
https://doi.org/10.1007/978-3-319-29279-3_11
Norman, J.R. (1937) LV.—Diagnoses of new Nototheniiform fishes collected by the "Discovery" Expedition. *Annals and Magazine of Natural History*, 20 (118), 475–476.
https://doi.org/10.1080/00222933708655368
Novillo, M., Moreira, E., Macchi, G. & Barrera-Oro, E. (2018) Reproductive biology in the Antarctic bathydraconid dragonfish *Parachaenichthys charcoti*. *Polar Biology*, 41, 2239–2248.
https://doi.org/10.1007/s00300-018-2359-5
Novillo, M., Moreira, E., Macchi, G. & Barrera-Oro, E. (2019) Reproductive effort in *Chaenocephalus aceratus* validated by gonadal histology: inshore sites serve as spawning grounds for some notothenioids. *Polar Biology*, 42, 1959–1972.
https://doi.org/10.1007/s00300-019-02571-8
Nybelin, O. (1947) Antarctic fishes. *Scientific Results of the Norwegian Antarctic Expeditions (1927-1931)*, 26, 1–76.
O'Brien, K.M., Crockett, E.L., Adams, B.J., Amsler, C.D., Appiah-Madson, H.J., Collins, A., Desvignes, T., Detrich, H.W., Distel, D.L., Eppley, S.M., Frable, B.W., Franz, N.M., Grim, J.M., Kocot, K.M., Mahon, A.R., Mayfield-Meyer, T.J., Mikucki, J.A., Moser, W.E., Schmull, M., Seid, C.A., Smith, C.R., Todgham, A.E. & Watkins-Colwell, G.J. (2022) The time is right for an Antarctic biorepository network. *Proceedings of the National Academy of Sciences*, 119 (50), e2212800119.
https://doi.org/10.1073/pnas.2212800119
O'Brien, K.M., Rix, A.S., Egginton, S., Farrell, A.P., Crockett, E.L., Schlauch, K., Woolsey, R., Hoffman, M. & Merriman, S. (2018) Cardiac mitochondrial metabolism may contribute to differences in thermal tolerance of red- and white-blooded Antarctic notothenioid fishes. *Journal of Experimental Biology*, 221 (15), jeb177816.
https://doi.org/10.1242/jeb.177816
Pollard, D. & DeConto, R.M. (2009) Modelling West Antarctic ice sheet growth and collapse through the past five million years. *Nature*, 458 (7236), 329–332.
https://doi.org/10.1038/nature07809
Postlethwait, J.H., Yan, Y., Desvignes, T., Allard, C., Titus, T., Le François, N.R. & Detrich III, H.W. (2016) Embryogenesis and early skeletogenesis in the antarctic bullhead notothen, *Notothenia coriiceps*. *Developmental Dynamics*, 245 (11), 1066–1080.
https://doi.org/10.1002/dvdy.24437
Provan, J. & Bennett, K.D. (2008) Phylogeographic insights into cryptic glacial refugia. *Trends in Ecology & Evolution*, 23 (10), 564–571.
https://doi.org/10.1016/j.tree.2008.06.010
Rambaut, A., Drummond, A.J., Xie, D., Baele, G. & Suchard, M.A. (2018) Posterior Summarization in Bayesian Phylogenetics Using Tracer 1.7. *Systematic Biology*, 67 (5), 901–904.
https://doi.org/10.1093/sysbio/syy032
Regan, C.T. (1913) The Antarctic Fishes of the Scottish National Antarctic Expedition. *Earth and Environmental Science Transactions of The Royal Society of Edinburgh*, 49 (2), 229–292.
https://doi.org/10.1017/S0080456800003951
Regan, C.T. (1914) Diagnoses of new marine fishes collected by the British Antarctic ("Terra Nova") Expedition. *Annals and magazine of Natural History*, Series 8, 13 (73), 11–17.
https://doi.org/10.1080/00222931408693450
Richardson, J. (1844) *Ichthyology of the Voyage of HMS Erebus & Terror, Under the Command of Captain Sir James Clark Ross.* E.W. Janson, London, 139 pp.
Riddle, M.J., Craven, M., Goldsworthy, P.M. & Carsey, F. (2007) A diverse benthic assemblage 100 km from open water under the Amery Ice Shelf, Antarctica. *Paleoceanography*, 22 (1).
https://doi.org/10.1029/2006PA001327
Sabaj, M.H. (2020) Codes for Natural History Collections in Ichthyology and Herpetology. *Copeia*, 108 (3), 593–669.
https://doi.org/10.1643/ASIHCODONS2020
Sabourenkov, E.N. & Appleyard, E. (2005) Scientific observations in CCAMLR fisheries–past, present and future. *CCAMLR Science*, 12, 81–98.
Saravia, J., Paschke, K., Oyarzún-Salazar, R., Cheng, C.-H.C., Navarro, J.M. & Vargas-Chacoff, L. (2021) Effects of warming rates on physiological and molecular components of response to CTMax heat stress in the Antarctic fish *Harpagifer antarcticus*. *Journal of Thermal Biology*, 99, 103021.
https://doi.org/10.1016/j.jtherbio.2021.103021
Sheiko, B.A. (2019) Comments on the nomenclature of genus-and family-series taxa of notothenioid fishes (Perciformes, Notothenioidei). *Bionomina*, 16 (1), 46–82.
https://doi.org/10.11646/bionomina.16.1.3
Skóra, K.E. (1995) *Acanthodraco dewitti* gen. et sp. n (Pisces, Bathydraconidae) from Admiral Bay (King George Island, South Shetland Islands, Antarctica). *Archive of fishery and marine research*, 42 (3), 283–289.

Sutter, J., Fischer, H., Grosfeld, K., Karlsson, N.B., Kleiner, T., Van Liefferinge, B. & Eisen, O. (2019) Modelling the Antarctic Ice Sheet across the mid-Pleistocene transition – implications for Oldest Ice. *The Cryosphere*, 13 (7), 2023–2041. https://doi.org/10.5194/tc-13-2023-2019

Trathan, P.N., Warwick-Evans, V., Young, E.F., Friedlaender, A., Kim, J.H. & Kokubun, N. (2022) The ecosystem approach to management of the Antarctic krill fishery - the "devils are in the detail" at small spatial and temporal scales. *Journal of Marine Systems*, 225, 103598. https://doi.org/10.1016/j.jmarsys.2021.103598

Vaillant, L.L. (1906) Sur une nouvelle espèce de Chaenichthys provenant de l'expédition antarctique francaise sous le commandement du Dr. Jean Charcot. *Bulletin du Muséum National d'Histoire Naturelle*, 5, 246–247. https://doi.org/10.5962/bhl.part.4096

Waite, E.R. (1916) Fishes. *Australasian Antarctic Expedition. Scientific Reports*, 3, 1–92.

Watters, G.M., Hinke, J.T. & Reiss, C.S. (2020) Long-term observations from Antarctica demonstrate that mismatched scales of fisheries management and predator-prey interaction lead to erroneous conclusions about precaution. *Scientific Reports*, 10 (1), 2314. https://doi.org/10.1038/s41598-020-59223-9

Westerhold, T., Marwan, N., Drury, A.J., Liebrand, D., Agnini, C., Anagnostou, E., Barnet, J.S.K., Bohaty, S.M., De Vleeschouwer, D., Florindo, F., Frederichs, T., Hodell, D.A., Holbourn, A.E., Kroon, D., Lauretano, V., Littler, K., Lourens, L.J., Lyle, M., Pälike, H., Röhl, U., Tian, J., Wilkens, R.H., Wilson, P.A. & Zachos, J.C. (2020) An astronomically dated record of Earth's climate and its predictability over the last 66 million years. *Science*, 369 (6509), 1383–1387. https://doi.org/10.1126/science.aba6853